SAPIENZA
University of Rome
Faculty of Pharmacy and Medicine

PhD in
Morphogenesis and Tissue Engineering

XXX Cycle
(A.A. 2016/2017)

Unravelling the role of NAADP/TPC2 Ca^{2+} signalling during angiogenesis and tumor progression

PhD student
Francesca Papacci

Tutor
Prof. Antonio Filippini

Coordinator
Prof. Sergio Adamo

Alla mia famiglia e a mio marito

INDEX

1. THE THESIS EXPLAINED

Nicotinic acid adenine dinucleotide phosphate (NAADP) mediated calcium (Ca^{2+}) signalling controls major cellular functions and involves an emerging family of intracellular channels specifically expressed on acidic compartments: Two-pore channels (TPCs). In particular, we have previously demonstrated that TPC2 isoform has a key role during angiogenesis and is likely involved in melanoma progression. Our earlier results were obtained using a selective membrane-permeant noncompetitive antagonist Ned-19 that is able to block NAADP- mediated Ca^{2+} signalling[1, 2].

In order to investigate a novel pharmacological tool able to interfere with the activity of TPC2 channel we have explored the potentiality of a natural flavonoid, Naringenin (Nar), in our models.

In accordance to electrophysiological evidences in a heterologous system, i.e. Arabidopsis vacuoles lacking endogenous TPCs, the present research has demonstrated that Nar dampens intracellular Ca^{2+} responses of human endothelial cells stimulated with VEGF, histamine or NAADP-AM, but not NAADP-independent stimuli, ATP and Angiopoietin-1. Moreover, Nar is able to impair angiogenesis *in vitro* and in an *in vivo* murine model.

On the basis of these and previous data we have also investigated Nar effects on B16 melanoma cells. We have observed that Nar impairs NAADP-controlled Ca^{2+} signalling (stimulated both directly and indirectly) and, interestingly, affects cells ability to proliferate/and or migrate. Furthermore, B16 melanoma cells capability to form vascular-like structures is impaired by Nar.

Our present data suggest that Nar inhibition of TPC2 activity and the observed inhibition of angiogenic response to VEGF are linked by impaired intracellular Ca^{2+} signalling in endothelial cells. In addition, Nar effects on B16 melanoma cells strengthen the hypothesis that TPC2 represent a potential target for the control of the progression of melanoma and possibly of other tumors. The relationship we describe in endothelial cells between Nar and

TPC2 is therefore likely to have wider implications representing a novel tool for experimental, and possibly even clinical, research purposes.

2.INTRODUCTION

2.2 Calcium signalling complexity in health and diseases

Calcium (Ca^{2+}) represents the most abundant and ubiquitous intracellular second messenger able to mediate different cell functions transducing several environmental signals into biological responses. Indeed, it's known that Ca^{2+} plays an important role in some physiological processes such as fertilization, development, differentiation, proliferation, contraction, secretion, exocytosis, metabolism, gene transcription, apoptosis [3, 4] and angiogenesis [1, 5]. Spatiotemporal changes in intracellular Ca^{2+} concentration are coordinated by the intrinsic linking between internal compartments and plasma membrane channels. Although the maintenance of intracellular Ca^{2+} homeostasis represents a pivotal aspect for cell survival different mechanisms have evolved aimed to regulate the Ca^{2+} removal from the cytoplasm extruding it across the cell plasma membrane or sequestering it in intracellular stores.

Plasma membrane Ca^{2+} ATPase (PMCA), Na^+/ Ca^{2+} exchanger (NCX) and $Na^+/ Ca^{2+}/ K^+$ (NCKX) represent the major proteins involved in withdrawing Ca^{2+} from the cytosol into extracellular medium. Instead, sarcoplasmic/endoplasmic reticulum Ca^{2+} ATPase (SERCA) pumps and ATPases closely related to SERCA contribute to sequestering Ca^{2+} in the sarco-endoplasmic reticulum and nuclear envelope, respectively. Furthermore, also mitochondria behave as buffers and stores Ca^{2+} in particular through the action of the inner mitochondrial membrane-spanning mitochondrial Ca^{2+} uniporter (MCU), mitochondrial Na^+/ Ca^{2+} exchanger and the permeability transition pore (PTP) [6]. Likewise, Ca^{2+} influx from extracellular space is mediated by channels, pumps and exchangers which control Ca^{2+} entry in response to stimuli such as membrane depolarization, stretch, noxious stimuli, extracellular agonists, intracellular messengers and depletion of internal compartments [4]. For example, the voltage-operated Ca^{2+} channels (VOCCs) are present in excitable cells plasma membrane; consequently to membrane depolarization these channels undergo conformational

changes that cause Ca^{2+} influx from the extracellular environment down an electrochemical gradient. Finally when intracellular stores are empty a process known as store-operated Ca^{2+} entry (SOCE) induces the activation of ORAI1/STIM1 complex that allows Ca^{2+} entry across the plasma membrane [6].

Instead, Ca^{2+} release from intracellular stores is controlled by Ca^{2+} itself or by different Ca^{2+} mobilizing messengers such as inositol-1,4,5-trisphosphate $(Ins(1,4,5)P_3)$, cyclic ADP ribose (cADPR), which mobilize Ca^{2+} from endoplasmic reticulum stores (ER) and nicotinic acid adenine dinucleotide phosphate (NAADP) which modulates Ca^{2+} release from acidic compartments such as endosomes and lysosomes [4] (Figure 1).
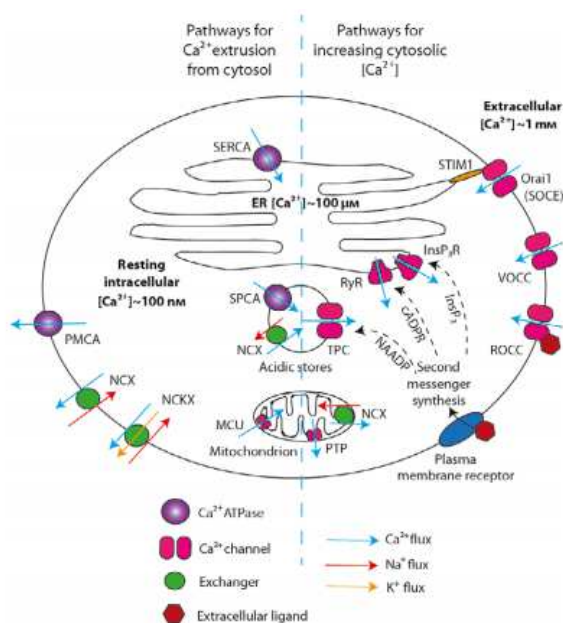
Parrington J. and Tunn R. Acta Physiol 2014, 211, 285-296

Figure 1. Overview of Ca^{+2} signalsome: dynamics, homeostasis and release.

Global Ca^{2+} increases that may be transient or sustained, highly localized or appear as waves or oscillations represent changes in cytosolic free Ca^{2+} that can be transduced by the cell in a signal able to specifically regulate cell processes. Ca^{2+} signalling complexity due to the numerous pathways in which Ca^{2+} is involved implies that Ca^{2+} signalling deregulation can be a characteristic of different pathological states, including cancer [7]. Ca^{2+} signalling alterations are not necessary for cancer initiation but represent a pivotal point for tumor progression because Ca^{2+} is involved in relevant biological cancer hallmarks such as the ability to avoid apoptosis, self–sufficiency in growth regulation, invasion and metastasis, unlimited replication potential, resistance to anti-mitotic and anti-angiogenic stimuli, (Figure 2) [8-12]. Ca^{2+} toolkit used by cancer cells is not different from that of non-malignant cells but there may be some key alterations. Compared to non-malignant cells, cancer cells may express Ca^{2+} channels, pumps, or their specific isoforms, not generally present in normal cells of the same cell type; they may have important changes in the level of the expression, modified cellular localization, post-translational modifications, that can induce altered activity, gene mutations or changes in activity or expression associated with specific cancer-relevant processes. Furthermore, these alterations can result in changes in Ca^{2+} flux across intracellular organelles or across the plasma membrane [11]. Although Ca^{2+} signalling represent a new recent field of research in oncology, understanding how targeting Ca^{2+} channels pumps or exchangers and the pathways regulated by them may represent a novel area of interest to develop drugs and oncological therapy aimed to contrast cancer progression.
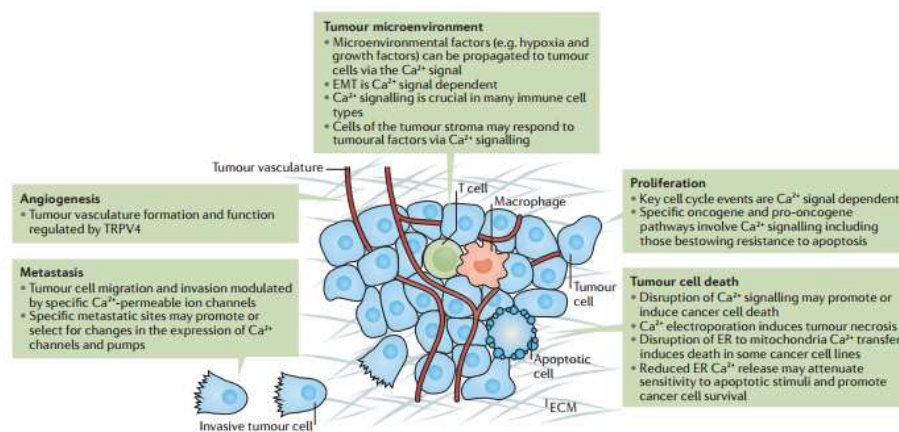
Monteith G. R. et al Nat Rev Cancer 2017, 17, 367-380

Figure 2. A summary of some cancer-associated processes and pathways in which Ca^{2+} is involved.

2.2 Calcium signalling pathway mediated by NAADP: the emerging role of Two-Pore Channels

NAADP is a potent second messenger able to mobilize Ca^{2+} from compartments different from those activated by IP_3 and cADPR. Initially discovered in sea urchin eggs [13] it was then confirmed in a wide range of cell types [14]. Further characterizations showed that NAADP was able to induce Ca^{2+} release from reserve granules (lysosomes-related organelles) and not from the ER suggesting that these organelles may operate as Ca^{2+} stores [15]. Synthesis of intracellular NAADP is still a matter of debate to be controversial but some ADP-ribosyl cyclases and the mammalin CD38 have been shown to catalyze NAADP formation in some cell types; this mechanism seems to be the only existing one in biological systems [14]. NAADP synthesis can be induced by cellular stimulation or

by activation of cell surface receptors to regulate a variety of processes such as fertilization, production of nitric oxide (NO) and glucose metabolism [14, 16].

The specificity of Ca^{2+} release from endolysosomal system induced by NAADP is still debated because it has been demonstrated that it can also mobilze Ca^{2+} from sarco-endoplasmic reticulum by directly activating RyRs. In particular, in cardiac and skeletal muscle, NAADP has been shown to be able to discharge Ca^{2+} through RyR activation [16-18]. In addition, NAADP can also elicit Ca^{2+} release from the same thapsigargin-sensitive pool that is sensible to IP_3 and cADPR [16, 19-22]. In sea urchin egg homogenate IP_3, cADPR and NAADP seem to be involved in Ca^{2+} release mechanisms of functionally and pharmacologically distinct organelles [23]; in intact cells, instead, an interaction between these messengers has been usually observed. Pharmacological approaches in sea urchin eggs using IP_3R and RyR antagonists showed that Ca^{2+} release induced by NAADP appeared as a diffusional gradient [24]. On the basis of these evidences a unified hypothesis known as "trigger hypothesis" was proposed. Ca^{2+} acidic stores may trigger a further Ca^{2+} release from ER by a mechanism dependent on functional IP_3Rs or RyRs. Local Ca^{2+} released from acidic compartments is amplified in a more globalized phenomenon that involves the larger and more extensive ER Ca^{2+} stores, event known as Ca^{2+}-induced Ca^{2+} release (CICR) [14], (Figure 3).
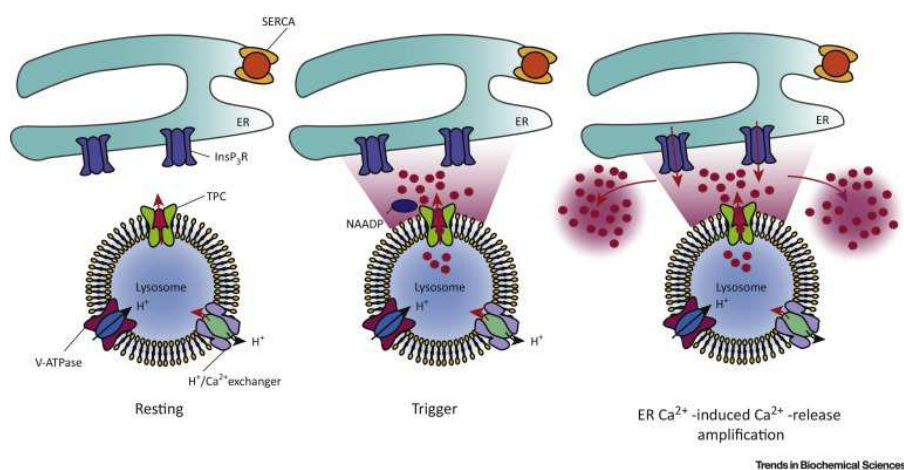
Raffaello A. et al Trends in Biochemical Sciences, 2016,41, 1035-1049

Figure 3. The unified "trigger hypothesis": from a local trigger to a more globalized phenomenon. NAADP induced Ca^{+2} release from acidic stores that causes a Ca^{+2} release from ER.

Different channels such as RyR1 [20], mucolipin 1 (TRPML1) [25] and TRPM2 [26], are proposed as molecular targets of NAADP Ca^{2+} fluxes, but the most accredited candidates are a family of ion channels named two-pore channels (TPCs) [27-29]. TPCs are members of the voltage-gated cation channels superfamily present both in endolysosomes and vacuoles; they represent the only family of Ca^{2+} release channels present in both plant and animal cells, (Figure 4a) [30]. TPCs comprise two repeats of a six-trasmembrane pore-forming domain [31] and are present in three different isoforms TPC1, TPC2 and TPC3. In human and mice there are the first and the second isoforms, while in many vertebrates, including chickens and rabbits, there is the third isoform [32].

TPCs localize to the endolysosomal system but their relative density is linked to the phase of maturation of the acidic organelles

and to the different pH. Indeed, TPC1 is generally expressed in recycling endosomes, early and late endosomes and lysosomes while TPC2 is predominantly localized into late endosomes and lysosomes, (Figure 4b) [33].

a
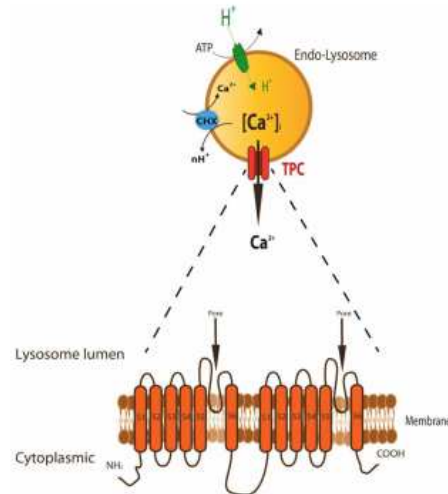
Parrington J. et al Int. J. Dev. Biol, 2015, 59:341-355

b
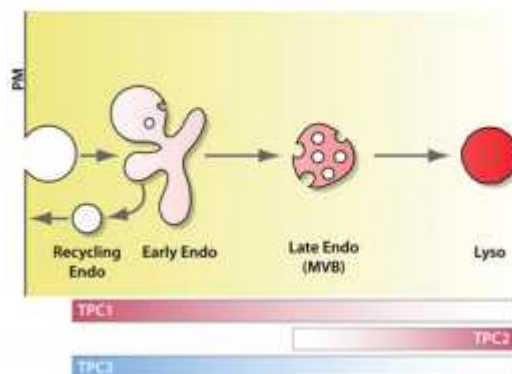
Morgan A. J. et al Biochem. J., 2011, 439, 349-374 [34]

Figure 4. [a] A schematic representation of endolysosomal membrane that shows TPCs transmembrane localization. **[b]** TPCs relative density linked to pH and endolysosomal system maturation.

Although both TPC1 and TPC2 activation are regulated by NAADP, TPC1 seems to be also activated by Ca^{2+}. Moreover, also ion conduction and permeability differ considerably. TPCs are permeable to a wide range of cations although biophysical data propose that TPC2 is slightly more selective for Ca^{2+} over K^+ than TPC1 and consequently able of discharging considerable quantities of Ca^{2+} from acidic compartments. It has been shown that TPC1 is also permeable to H^+ and for this reason it may be involved in the regulation of lysosomal and cytosolic pH. These differences in gating and ion conducting properties suggest that TPC1 and TPC2 may accomplish complementary physiologal roles as Ca^{2+} release channels of endo-lysosomal compartments [35].

Several studies support the evidence that TPCs mediate Ca^{2+} release evoked by NAADP [28, 35, 36] from acidic stores although has been reported evidences indicating that TPCs are not activated by NAADP but rather than $PI(3,5)P_2$ [37, 38]. A very recently work by Ruas and co-workers shows that NAADP–induced Ca^{2+} release were significantly impaired in cells TPC1 and TPC2 double knock out corroborating the hypothesis that both TPC1 and TPC2 are NAADP targets [39]. Finally, the possible explication of such contrasting data is that NAADP may not directly interact with TPCs, but through an accessory binding protein [40, 41] element that might be lost in the different experimental conditions [42].

2.3 Role of NAADP and TPCs in pathophysiological processes

Ca^{2+} signalling from TPCs evoked by NAADP is involved in different physiological processes including cellular differentiation, muscle contraction, endothelial activation, membrane trafficking, autophagy, nutrient sensing exocytosis, fertilization and embryogenesis, cytokinesis [42] and pigmentation [43-45]. Furthermore, in our laboratory we have recently demonstrated the emerging role of NAADP elicited pathway, in particular mediated

by TPC2, in angiogenesis. Indeed, in angiogenic process Vascular Endothelial Growth Factor (VEGF) signalling pathway play a pivotal role. Activation of Vascular Endothelial Growth Factor receptor 2 (VEGFR2) results in an increase in intracellular free Ca^{2+} mediated by NAADP that controls proliferation, migration and sprouting of endothelial cells (ECs). *In vitro* experiments in human umbilical vein endothelial cells (HUVECs), using a selective NAADP antagonist (Ned-19) or anti-TPC2 shRNA, showed a drastic inhibition of angiogenesis due to the significant reduction of VEGF-induced intracellular Ca^{2+} mobilization. Moreover, in *in vivo* experiments Ned-19 inhibited VEGF-induced vessels formation in matrigel plugs and accordingly in TPC2 knockout mice, but not TPC1 knockout mice, VEGF-induced vessels formation in matrigel plugs failed to occur [1].

Interestingly, recent studies reported the emerging role of TPCs in several pathologies such as myocardial ischemia [46], Parkinson's disease [47] and Ebola virus infection [48].

Recently TPCs mediated Ca^{2+} signalling has been described also in cancer. Indeed, a genetic analysis aimed to indentify genetic factors implicated in development and metastasis of human oral squamous carcinoma showed an over-expression of TPC2 gene as a possible driver of the amplification of 11q13 genomic region detected in distinct tumors but the mechanism that links TPC2 overexpression to changes in growth and metastatic potential still remains unclear.

Moreover, studies about the relationship between genes involved in skin pigmentation and the tendency for malignant melanoma have shown the possible correlation between cancer and TPC2. TPC2 gene polymorphisms has been identified as potential risk factors in this pathology. Furthermore, melanosomes are modified lysosomes and changes in TPC2 expression or function induces abnormalities on melanocytes biology that could enhance tumorigenity [49]. Involvement of NAADP-mediated responses in melanoma progression have been demonstrated also in my laboratory. Indeed, in *in vitro* experiments we have shown that VEGF-dependent Ca^{2+}

signalling is significantly reduced in B16 murine melanoma cells treated with NAADP-inhibitor Ned-19 and also in *in vivo* experiments in mice we have demonstrated a significant reduction of tumor growth and metastasis formation after four weeks of intraperitoneal Ned- 19 treatment [2]. In addition, data from Nguyen and co-workers indicate TPCs as possible targets of invasive cancers. In a very recent article they have shown that TPCs inhibition impairs migration and adhesion of T24 (bladder cancer), HUH7(hepatocarcinoma) and 4T1 (breast cancer) cancer cells *in vitro* and metastasis formation in a *in vivo* mouse model as result of altered integrin trafficking in the endolysosomal compartment [50].

The biological relevance of TPCs-mediated signalling in diseases, and in particular in cancer, make them possible targets for drugs development aimed to fight cancer development and progression.

2.4 Biological properties of flavonoids: focus on Naringenin

Flavonoids have aroused researchers interest for their indisputable biological properties supported by epidemiological studies that propose a direct link between the consumption of food rich in flavonoids and poor in fatty acids and a decreased risk of certain diseases in humans such as cardiovascular diseases, diabetes and cancer. Due to their antioxidants properties flavonoids seem to have also a pivotal role in the aging process, tissue damage and inflammatory processes [51]. Moreover, they exert a potential anti-invasive and/or anti-metastatic activities in a wide range of cancer types such as brain, thyroid, lung, prostate, ovarian, cervical, oral, hypopharyngeal, breast, liver, biliary tract, gastric, pancreatic, intestinal colon, renal and epidermal cancers, melanoma, fibrosarcoma, osteosarcoma and Kaposi's sarcoma, (Figure 5) [52].
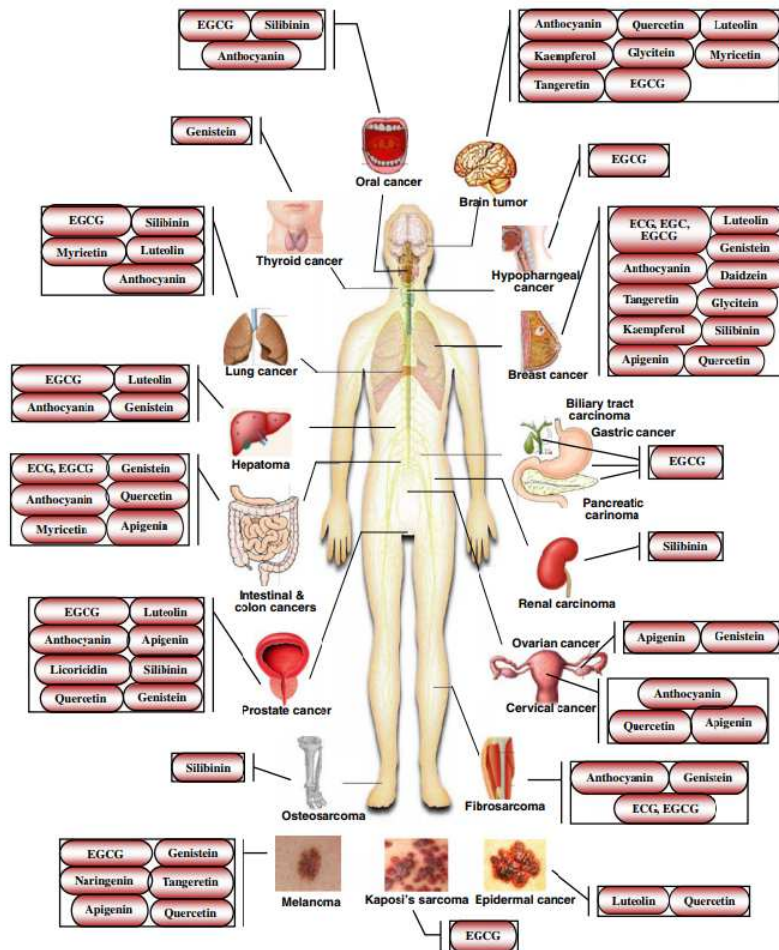
Weng C. J. and Yen G. C. Cancer Metastasis Rev, 2012, 31: 323-351.

Figure 5. Overview of flavonoids with anti-invasive and/or anti-metastatic properties in the fight of a variety of cancer types.

Naringenin (Nar) (5,7-dihydroxy-2-(4-hydroxyphenyl)chroman-4-one) is one of the main flavonoids present in human diet, (Figure 6).
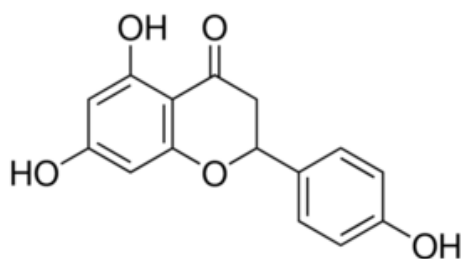
Figure 6. Chemical structure of Naringenin.

Evidences from epidemiological reports showed that the consumption of vegetables and fruit with a high Nar content, such as citruses and tomatoes or their food products, correlate with a reduced incidence of metabolic and chronic-degenerative diseases [53, 54]. Several *in vitro* studies have shown that Nar interacts with many cellular pathways, point out its properties as an antioxidant, antinflammatory, chemopreventive an antidegenerative agent [55]. In addition, it has been shown that Nar is able to exert anti-angiogenic effects *in vitro* impairing endothelial cell proliferation, survival, migration and capillary-like structures formation of HUVECs and *in vivo* reducing neovascularization in an avian chorio-allantoid membrane model [56]. Furthermore, in rats nourished with high-cholesterol diet Nar is able to lower plasma and hepatic cholesterol concentrations by suppressing HMG-CoA reductase and ACAT [57]. The potential of Nar and its precursor naringin emerged from pre-clinical studies which described their activity in treatment of metabolic and cardiovascular disorders such as hyperlipidemia, hypertension, cardiac toxicity, hyperglycemia and diabetes, hepatic steatosis, atherosclerosis [54] and cancer [55]. Indeed, Nar chemopreventive and anticancer

activity has been described; it has been shown that Nar is able to block the progression and the formation of metastasis in different experimental models of oral [58], melanoma [59], breast [60, 61], colon[62], lung [63], and liver [64] cancers. It seems to act by upregulating many different cell survival proteins or arresting cell cycle, by inducing p53-dependent apoptosis or inhibiting inflammatory processes and, in some cases, by exploiting all of these mechanisms [52, 65, 66]. Interestingly, it is known that Nar affects also the activity of different calcium-activated or calcium-permeable ion channels. Nar 100 µM induces a threefold increase in the currents mediated by large conductance Ca^{2+}-activated K^+ (BKCa) channels, which can be closely correlated with the significant vasorelaxant effect mediated by Nar on rat endothelium-denuded vessels [67]. Moreover, the relaxant effect of Nar on rat colon smooth muscle has been attributed to the direct activation of BKCa channels, resulting in hyperpolarization of smooth muscle cells, which in turn reduces the Ca^{2+} influx through voltage-dependent calcium channels [68]. Furthermore, Nar is a powerful inhibitor of the melastatin-related transient receptor potential TRPM3 belonging to the TRP family, a calcium-permeable non-selective cation channel expressed in various neural and non-neural tissues, activated by neurosteroids and heat [69]. Since TRPM3-deficient mice display an impaired perception of noxious heat, the inhibition of TRPM3 may represent a novel tool for analgesic therapy [70]. Another member of the TRP family, TRPP2 or polycystin-2, a Ca^{2+}-permeable non-selective cation channel located in the ER and in the primary cilium, is modulated by Nar concentrations ranging from 50 to 200 µM. This channel is implicated in the development of autosomal dominant polycystic kidney disease (ADPKD). It has been suggested that Nar may activate TRPP2 to cause Ca^{2+} influx and a decrease in cellular proliferation, thereby providing a novel therapeutic approach to ADPKD [71]. Despite the fullness of evidence on Nar efficacy, an exhaustive explanation of its mechanism of action is still lacking,
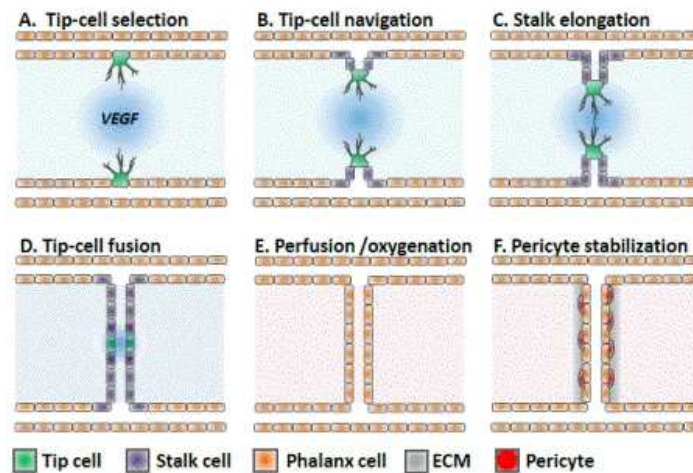
as is the experimental evidence needed to bridge the gap between multiple cellular targets and biological response.

2.5 Physiological angiogenesis versus tumoral angiogenesis: a general overview

Angiogenesis is the physiological process that foresees the formation of the new blood vessels from pre-existing ones. Although angiogenesis is a phenomenon which occurs throughout life, in the adult the vasculature is generally quiescent and physiological angiogenesis is restricted to some adult tissues that require regeneration or restructuring (including female reproductive organs or injured tissue) [72, 73].

Angiogenesis is characterized by two different mechanisms: sprouting and splitting (or intussusceptive angiogenesis).

In sprouting angiogenesis enzymatic mechanisms induce degradation of capillary basement membrane, ECs proliferate and migrate, there is a tube formation, vessel fusion and pruning and the stabilization of pericytes. This process begins when tissues are poorly perfused and critical hypoxic levels require blood vessels formation aimed to meet the metabolic needs of parenchymal cells. As a response to the hypoxic conditions several parenchymal cells produce VEGF, a key factor that plays a pivotal role during early stages of angiogenesis. The sprouting process is guided by a tip cell which displays filopodia that moves toward VEGF gradient concentration through VEGF-VEGFR2 interaction. Tip cell determination is controlled by the cell-cell signalling pathway Delta-Notch that is activated by interaction of VEGF with ECs. Capillary sprout elongation is determined by contraction of filaments within the filopodia that draw the tip cell along toward the VEGF source causing consequent proliferation of endothelial stalk cells [72].

A. Tip-cell selection   B. Tip-cell navigation   C. Stalk elongation

VEGF

D. Tip-cell fusion   E. Perfusion /oxygenation   F. Pericyte stabilization

Tip cell   Stalk cell   Phalanx cell   ECM   Pericyte

Adair T.H., Montani J.P. Angiogenesis. San Rafael (CA): Morgan & Claypool Life Sciences; 2010. Chapter 1.

Figure 7. Different steps which characterize sprouting angiogenesis.

Convergence of tip cells from different capillary sprouts toward VEGF stimulus source induces the fusion of these cells causing the formation of a continuous lumen perfusible by oxygenated blood. Finally, consequent involvement of pericytes and the extracellular matrix deposition, including the arrest of ECs proliferation, contributes to the capillary maturation and stabilization [72] (Figure 7).

Pro-angiogenic factors (for example VEGF, angiopoietins, epidermal growth factor (EGF), transforming growth factor-α (TGF-α), fibroblast growth factor (FGF)) and anti-angiogenic factors (for example angiostatin, endostatin, thrombospondin) contribute to the correct functioning of the angiogenic process [74].

Splitting angiogenesis or intussusceptive angiogenesis, instead, is a phenomenon that plays a key role in the growth and remodelling of most vascular beds, including those of the tumor. During this process a single vessel splits in two different vessels. Invagination of the capillary walls into the vascular lumen induces the formation of intraluminal tissue pillars. The vessel wall of the opposite sides of a vessel extend toward each other forming an intraluminal pillar. In the following phases of the splitting, reorganization of the interendothelial junctions and the formation of the core of the pillar occur and afterwards pericytes and myofibroblsts invade the pillar. Finally fusion of different pillars induces the splitting of the initial capillary in two different ones, (Figure 8) [75].
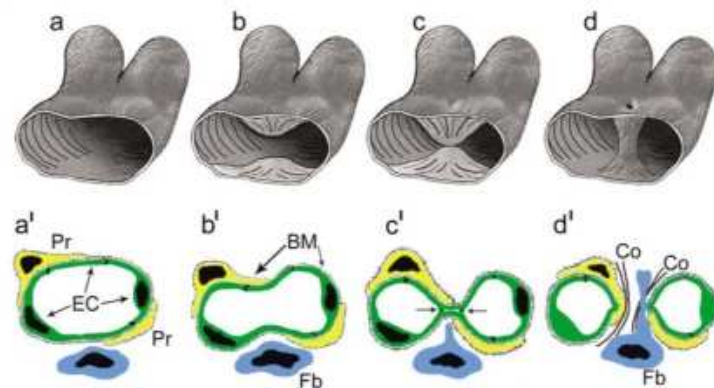

Adair T.H., Montani J.P. Angiogenesis. San Rafael (CA): Morgan & Claypool Life Sciences; 2010. Chapter 1.

Figure 8. Representation in three dimensions (a-d) and two dimentions (a'-d') of different steps of intussusceotive angiogenesis. Endothelial cells (EC); basement membrane (BM); fibroblasts (Fb); pericytes (Pr); collagen fibrils (Co).

Moreover, intussusceptive angiogenesis has been recognized in three different forms: intussusceptive microvascular growth,

intussusceptive arborisation and intussusceptive branching remodelling [75, 76].

Intussusceptive angiogenesis seems to be a fast and efficient process that occurs in pre-existing vascular systems previously formed by vasculogenesis or sprouting angiogenesis without interfering with the local physiological conditions. Indeed, this type of angiogenesis occurs throughout life but plays a pivotal role during embryonic vascular formation in a context in which growth is fast and resources are limited [72]. Furthermore, splitting angiogenesis seems to be regulated both by hemodynamic forces and pro- angiogenic factors such as VEGF, angiopoietins, FGF and PDGFβ [75].

In general, loss of the appropriate balance between pro- and anti- angiogenic factors induces abnormalities in physiological angiogenic process toward a pathological angiogenesis, phenomenon known as "angiogenic switch" [73]. In cancer, for example, angiogenesis has a key role. Indeed tumor vessels supply tumor with oxygen, nutrients and subsequently remove waste. When tumors arise in a well vascularized region co-option of pre-existing vessels might be exploited. On the contrary, angiogenesis or the formation of new blood vessels from a pre-existing system occurs to guarantee tumor expansion. In this context the creation of a pro-angiogenic environment promotes the induction of growth vascular. Tumor secrete growth factors that produce a chemotactive gradient able to recruit ECs and perycites while matrix metalloproteinases generate remodelling of extracellular matrix aimed to facilitate migration and vascular morphogenesis [77].

Tumor blood vessels are architecturally different to the normal counterpart and show some characteristic hallmarks. There is not a specific organization in venules, arterioles and capillaries but blood vessels are usually chaotic, irregular, dilated, tortuous and can have dead end. The vascular system is leaky and haemorrhagic and in addition tumor vessels may have cancer cells integrated in the

Francesca Papacci

vessel wall. Moreover, blood perfusion may be irregular and slow, (Figure 9) [73].

a   b
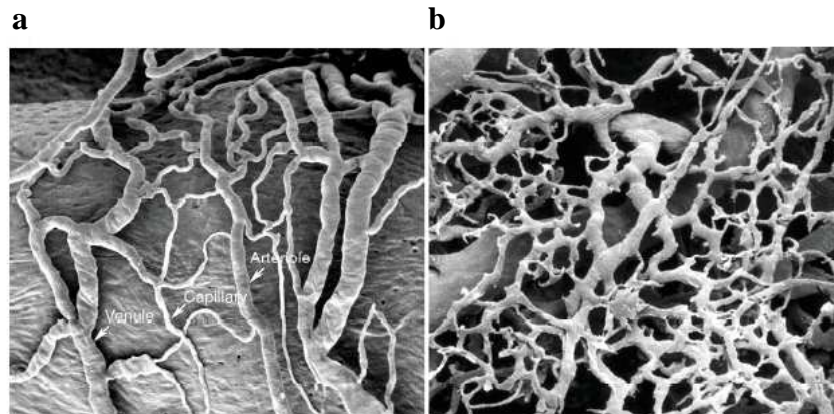
Modified from McDonald D.M. and Choyke P.L. Nat Med 2003, 9(6):713-25

Figure 9. Representative microscopic imaging of normal [a] and tumor vasculature [b]. [a] In normal blood vessels it is possible to observe a precise vascular network organization in arterioles, capillaries and venules. [b] Tumor blood vessels appear chaotic and not hierarchically organized [78].

Recently, several evidences show alternative mechanisms through which vascular supply can be formed in solid tumors, as represented in Figure 10. Co-option process foresees that tumors adopt pre-existing blood vasculature of the surrounding environment. In vascular mimicry, instead, aggressive tumor cells themselves, rather than endothelial cells, form capillary-like structures perfusible by blood able to provide support to cancer growth [79]. Initially discovered in melanoma, additional studies have demonstrated that several aggressive cancers such as some sarcomas, carcinomas or gliomas can display vascular mimicry [80, 81].
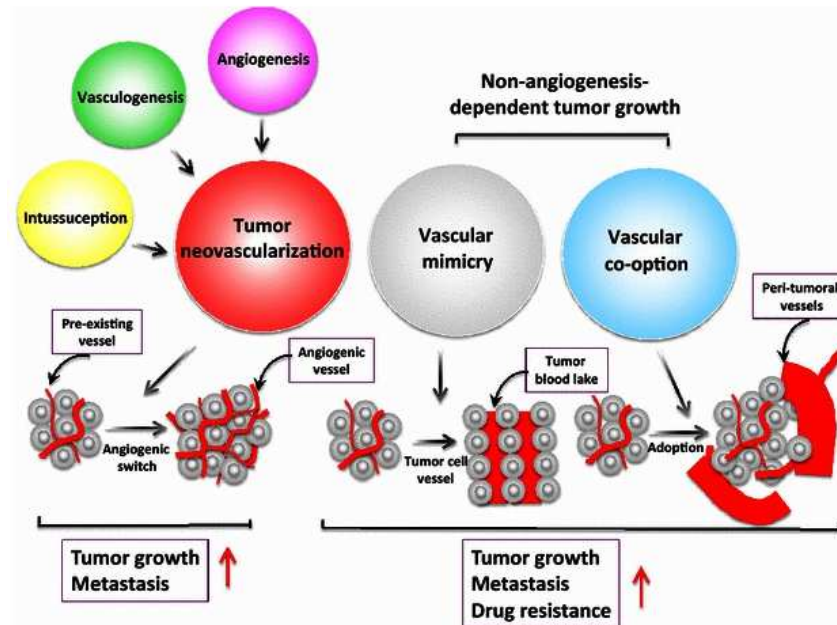
Cao Y. Chin J Cancer, 2016, 35:21

Figure 10. Different mechanisms exploited by solid tumors in order to provide blood supply supporting tumor growth, metastasis and drug resistance.

3. AIMS

In our previous studies we have demonstrated the emerging role of Two-Pore Channel 2 in angiogenesis and its likely involvement in melanoma progression. Indeed, we have described that HUVECs treated with the NAADP inhibitor Ned-19 or anti-TPC2 shRNA showed a drastic inhibition of angiogenesis due to the significant reduction of VEGF-induced intracellular Ca^{2+} mobilization. Moreover, in *in vivo* experiments Ned-19 inhibits VEGF-induced vessels formation in matrigel plugs and in TPC2 knockout mice, but not TPC1 knockout mice, VEGF-induced vessels formation in matrigel plugs failed to occur [1]. Furthermore, we have also demonstrated that Ned-19 is able to block growth, migration, adhesivity and VEGFR2 expression in B16 melanoma cells *in* vitro and tumor growth, metastasis formation and vascularization *in vivo*. Collectively, these observations propose NAADP/TPC2 signalling pathway as a key point not only for neoangiogenesis but also for the direct contol of tumor cells [2].

On this basis our laboratory is presently engaged in a number of experimental approaches with the ultimate aim of assessing whether TPC2 can be a suitable target for potential melanoma therapy. My specific contribution to this aim has been characterize a novel pharmacological tool exploring the potentiality of a natural flavonoid, Naringenin, in our models.

To this purpose we have focused our attention on Nar ability to modulate TPCs activity, given that Nar interferes different Ca^{2+} channels [67-71], in order to investigate its effects on VEGF-dependent angiogenesis and in melanoma behavior.

In particular the aims of this work are:

- In HUVECs : to evaluate Nar effects on NAADP-controlled Ca^{2+} responses through calcium imaging experiments and investigate Nar effects on VEGF-dependent angiogenesis *in vitro* and *in vivo*.

- In B16 melanoma cells: to evaluate Nar effects on NAADP-controlled Ca^{2+} responses through calcium imaging experiments and to investigate Nar effects on biological cancer processes such

as migration, proliferation and non-angiogenic vasculogenic mimicry.

4. RESULTS AND DISCUSSION

4.1 Naringenin affects the activity of the human TPCs directly impairing hTPC2 functional activity and decreasing hTPC1 activity

Mature plant cells have a particular intracellular compartment that is lacking in animal cells: the vacuole. Its large dimension and its easy isolation allow researchers to study it using patch-clamp techinique. Through this method it is possible to isolate a specific small patch of a membrane and precisely detect the current flowing through a single ion channel. Interestingly, in this way is possible to exploit *A. Thaliana* vacuole as a novel heterologous system for the expression and functional characterization of animal intracellular channels and transporters [82].

In collaboration with Armando Carpaneto group from CNR of Genoa, we have employed this heterologus system to assess the ability of Nar to bind and regulate the activity of human TPC2 (hTPC2). Isolated protoplasts of a mutant *A. thaliana*, lacking endogenous TPCs, were transiently transformed with hTPC2 equipped with an EGFP fused to its C-terminus [83]; we applied the patch-clamp technique to vacuoles in which GFP fluorescence was clearly detectable on the tonoplast. The addition of 330 nM $PI(3,5)P_2$ in the external (cytosolic) solution induced robust hTPC2-mediated currents, as shown in Figure 1a where stationary currents recorded at +40 mV were plotted versus time. When 500 μM Nar was also added in the cytosolic solution a strong decrease in the activity of hTPC2 currents was evident. Figure 1b shows control and recovery currents (ΔI) recorded in the presence of $PI(3,5)P_2$ subtracted by the correspondent background recorded without the phosphoinositide. Upon Nar application, currents were drastically reduced at both +40 and −40 mV voltages. Even if recorded in symmetrical concentration of sodium, due to a voltage-dependent block by cytosolic magnesium [84] the currents at +40 mV were smaller than those recorded at −40 mV. Interestingly,

Nar inhibition was fully reversible (Figure 1b). The dose-response was well described by a Michaelis-Menten hyperbolic function (Figure 1c), with apparent affinity constants of 180 ± 20 μM at $+40$ mV and of 240 ± 40 μM at -40 mV, therefore not significantly different.
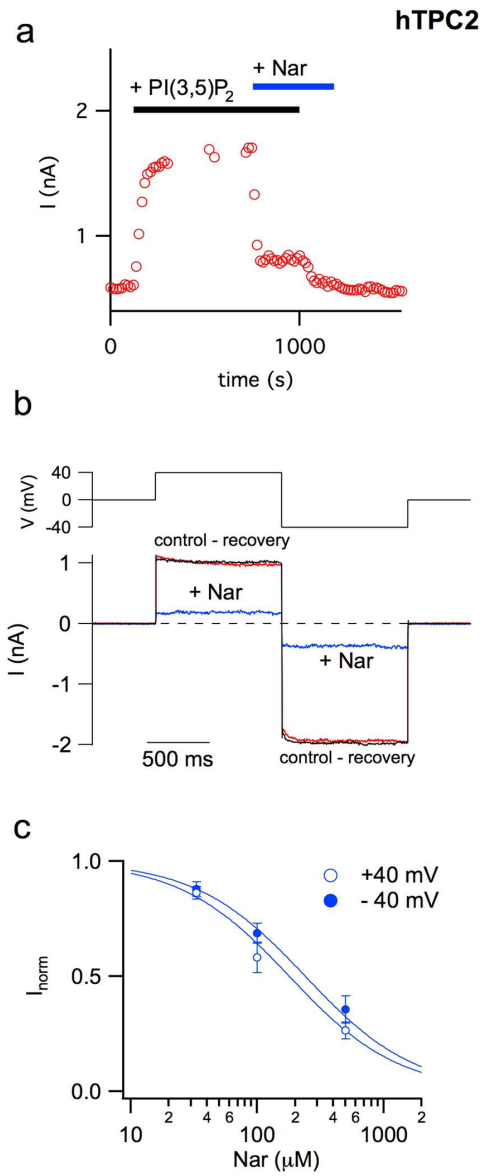
Figure 1. Naringenin inhibits the activity of the human TPC2 channel. (**a**) Time course of current amplitude recorded in response to bath application of 330 nM PI(3,5)P$_2$ (upper black bar) before and after adding 500 μM Nar (upper blue bar). Each point represents the steady-state current at +40 mV. (**b**) Currents

mediated by hTPC2 and induced by the application of 330 nM $PI(3,5)P_2$ in the cytosolic bath solution were recorded at $+40$ and -40 mV (shown in the upper voltage profile) in the absence or presence of 500 μM cytosolic Nar. For the sake of clarity, background currents in the absence of the phosphoinositide were directly subtracted. (**c**) Dose–response analysis of Nar inhibition. I_{norm}, the normalised current, was obtained by the ratio of currents recorded respectively in the presence and absence of cytosolic Nar. Both at $+40$ and -40 mV, normalised currents at different Nar concentrations were fitted with a Michaelis–Menten function (continuous lines). Data from 3 (Nar33 μM), 6 (Nar 100 μM) and 9 (Nar 500 μM) different vacuoles were shown as mean $\pm$ s.e.m. Values at positive and negative voltages, at a defined Nar concentration, were not significant ($P > 0.2$); values at different Nar concentrations and at a defined voltage ($+40$ or -40 mV), were statistically significant (at least $P < 0.01$).

We wondered if Nar could modulate the other member of the TPC family in humans, namely hTPC1. We therefore performed a similar approach as for hTPC2 and expressed hTPC1 fused to an EGFP at its C-terminus in *Arabidopsis Thaliana* vacuoles lacking the endogenous TPC1. Suppl. Figure 1a, left panel, shows that the background currents recorded in the absence of $PI(3,5)P_2$ are very small in comparison to those elicited by the addition of the phosphoinositide (right panel). We chose a concentration of $PI(3,5)P_2$ equal to 90 nM and therefore near to the saturation value since the apparent binding constant in this experimental condition was about 20 nM [85]; in comparison the affinity binding constant of $PI(3,5)P_2$ for hTPC2 is about 140 nM [83]. The current-voltage relationship in the absence (empty symbols) and in the presence (filled symbols) of $PI(3,5)P_2$ was plotted in Suppl. Figure 1b. In a recent paper [85] we demonstrated that the functionality of hTPC1 was strongly affected by both cytosolic and luminal Ca^{2+}, namely an increase in cytosolic and luminal Ca^{2+} induced an increase and a decrease of the activity of the channel, respectively.
Here, our standard pipette and ionic bath solutions (see Materials and Methods) allowed us to record hTPC1-mediated currents at both negative and positive potentials and therefore to evaluate the effect of Nar at different voltages. In Suppl. Figure 1b, at positive voltages, a voltage dependent inhibition of the hTPC1-induced

currents due to the presence of cytosolic magnesium was also apparent [85]; a similar effect was recorded for hTPC2 in Figure 1b and by other authors [84]. Figure 2a showed that the addition to the cytosolic solution of 500 μM Nar (trace 2) induced a significant decrease of hTPC1-elicited currents (trace 1) at both negative and positive voltages and had almost no effect in control conditions (compare trace 3 and 4). The inhibition of hTPC1 by Nar was quantified in the histogram of Figure 2b; the effect was not voltage-dependent. Moreover, we verified that Nar decreased the activity of the endogenous *Arabidopsis* TPC1 (Suppl. Figure 2) showing that the inhibition of TPC channels by Nar was a mechanism conserved during evolution.

All supplementary figures are showed in the appendix of the thesis.
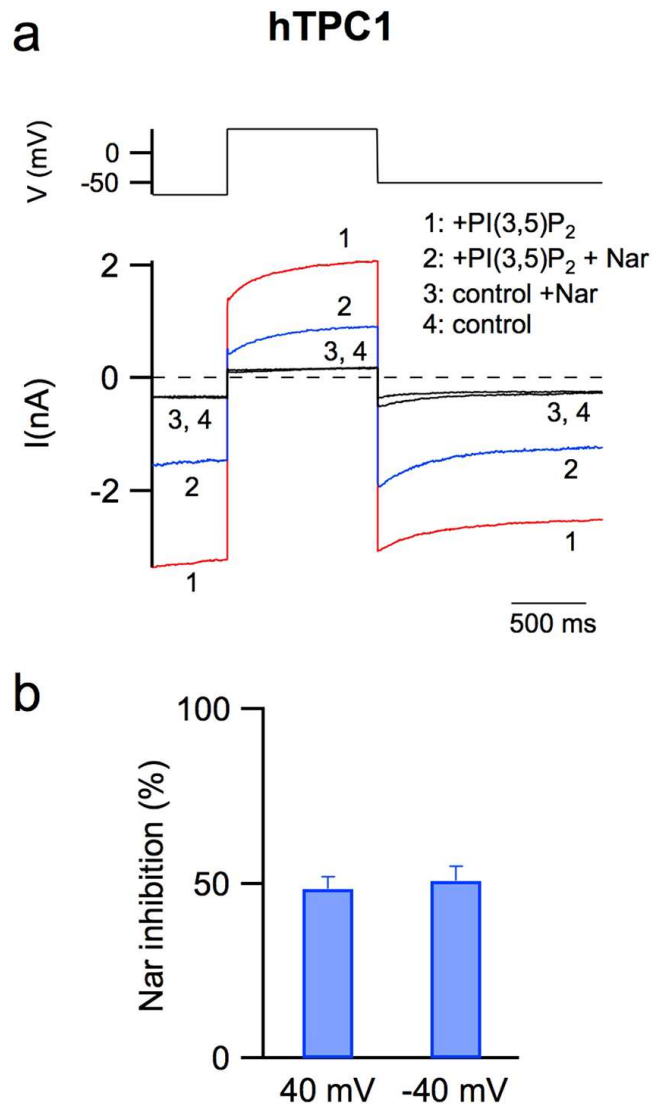
**Figure 2.** The activity of the human TPC1 channel is inhibited by Naringenin. (**a**) Currents (lower panel) recorded in control conditions (trace 4) or adding in the cytosolic bath solution: 90 nM PI(3,5)P$_2$ (trace 1), 90 nM PI(3,5)P$_2$ and 500 μM Nar (trace 2), 500 μM Nar (trace 3). In the upper panel the voltage profile is shown. (**b**) Percentage of current inhibition induced by 500 μM Nar added in the

cytosolic solution at -40 and $+40$ mV. Data from 6 different vacuoles, shown as mean $\pm$s.e.m., were not statistically significant ($P > 0.6$).

4.2 Naringenin significantly inhibits VEGF-dependent calcium mobilization in a dose-dependent manner

In HUVECs, we have previously demonstrated that VEGF-dependent Ca^{2+} mobilization evoked by NAADP is impaired pretreating cells with Ned-19 (a noncompetitive antagonist of NAADP) [1]. In order to evaluate the possible inhibitory effect of Nar on the regulation of VEGF-dependent Ca^{2+} signalling in human cells, calcium imaging experiments were performed pretreating HUVECs for 30 min with different concentrations of Nar and stimulating them with 100 ng/ml VEGF. Figure 3a,b shows that Ca^{2+} mobilization was significantly reduced in a dose-dependent manner without affecting VEGFR2 phosphorylation at Tyr1175 demonstrating that the inhibition of the responses occurs downstream of the receptor , (Figure 4). Furthermore, opting for 1000 µM Nar, for its highest effect, we have analyzed the specificity of this response for NAADP/TPC2- dependent Ca^{2+} signalling using a positive and a negative control. Bar charts in Figure 3c,d show that Nar fails to block Ca^{2+} response to ATP, known to be IP_3-dependent, but blocks histamine-evoked Ca^{2+} release known to be NAADP/TPC2-dependent [86]. These data are a strong indication that Nar is able to reduce Ca^{2+} release inhibiting hTPC2. Finally, to better correlate the specific inhibitory effect of Nar treatment on TPC2, calcium imaging experiments with the direct channel activator were performed. HUVECs Ca^{2+} mobilization in response to 500 nM NAADP-AM was significantly impaired pretreating cells with 500 µM or 1000 µM Nar. These set of experiments were accomplished in a Ca^{2+} free buffer to tightly evaluate the intracellular Ca^{2+} involvement alone thus limiting possible off-target responses (Figure 3e).

Taken as a whole, these data strongly suggest a direct effect of Nar on TPC2 given that it affects specifically Ca^{2+} released from acidic intracellular compartments.
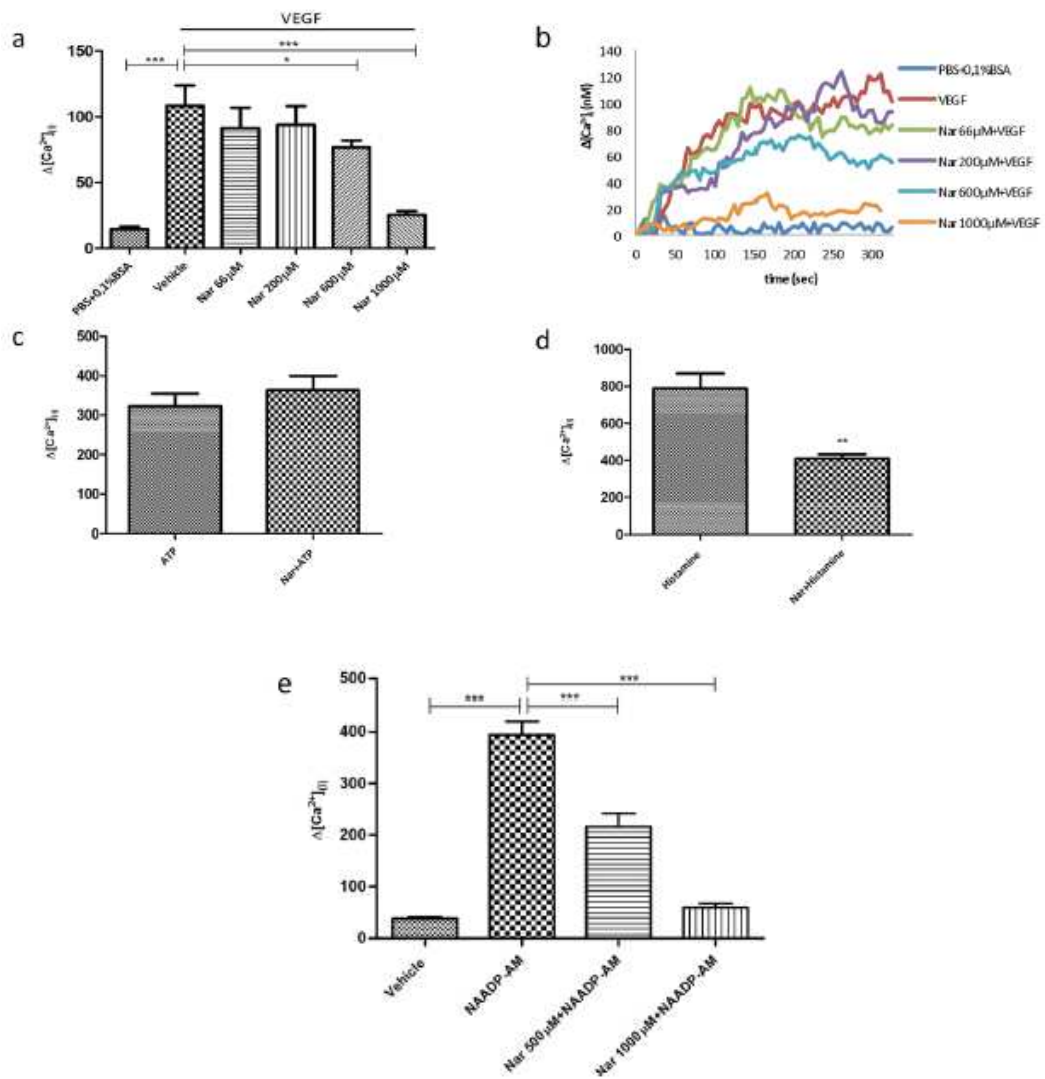
Figure 3. VEGF and NAADP-AM-dependent Ca^{2+} mobilization from acidic stores is inhibited by Naringenin. Live imaging in single FURA-2AM loaded

cells. (a,b) HUVECs were pretreated for 30 min with different concentrations of Nar and then stimulated with 100 ng/ml VEGF; (a) Bar chart showing maximum Ca^{2+} concentrations; (b) Changes in Ca^{2+} levels shown as representative traces. (c,d) Cells were pretreated with 1000 μM Nar for 30 min and then stimulated with (c) 10 μM ATP (negative control) or (d) 100 μM histamine (positive control). (e) Cells were pretreated with 500 μM or 1000 μM Nar and then stimulated with 500 nM NAADP-AM. Data in bar charts were from 3 independent experiments, $n = 41$–180 cells. $*P < 0.05$; $**P < 0.01$; $***P < 0.001$.
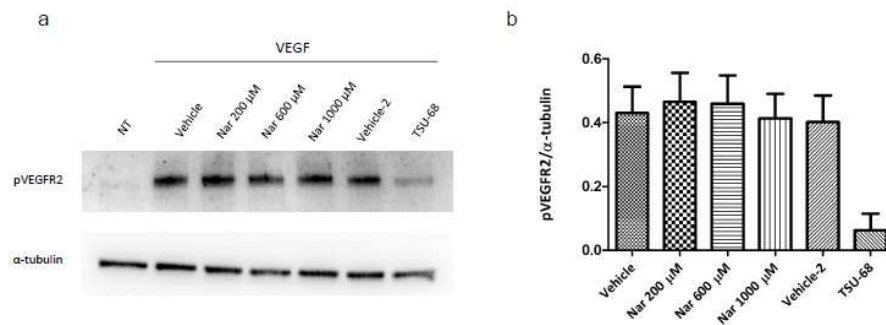
Figure 4. Phosphorylation state of VEGFR2 at Tyr1175, evaluated by western blot in untreated (NT) or VEGF-treated HUVECs. (a) Cells were preincubated with Nar (200 μM, 600 μM and 1000 μM) or vehicle for 30 min, or with TSU-68 (2,1 μM), or its control (vehicle-2) for 1h. Samples were then stimulated with 100 ng/ml VEGF for 15 min. The intensity of pVEGFR2 bands was quantified and normalized to α-tubulin content. (b) Data in bar chart represent mean ± s.e.m. from three independent experiments. As apparent, VEGF-induced receptor phosphorylation is significantly inhibited by TSU-68 but not by Nar.

4.3 Naringenin impairs VEGF-induced angiogenic process *in vitro* and *in vivo*

Li et al recently have demonstrated the antiangiogenic effects of Nar on HUVECs *in vitro* and in the avian chorio-allantoid membrane model *in vivo*. Although its antiangiogenic effects have

been reported to involve impairment of estrogen-related receptor α (ERR α) and VEGF secretion, the specific pathway involved has yet to be understood [56]. Previously, we have demonstrated that NAADP-mediated Ca^{2+} signalling has a key role in the regulation of *in vitro* and *in vivo* angiogenesis. VEGF-induced angiogenesis was inhibited by Ned-19 *in vitro* and in an established *in vivo* murine model [1]. In order to explore the anti-angiogenic effects of Nar we have evaluated VEGF-dependent angiogenesis *in vitro* and *in vivo*.

HUVECs have the ability to form capillary-like tubes *in vitro*, characteristic that is commonly considered as representative of later, differentiative, steps of angiogenesis. In this way exploiting this assay it is possible to analyze the pro or anti-angiogenic effects of a compound. ECs plated onto matrigel matrix adhere, migrate and, within a few hours, differentiate into capillary- like structures.

Figure 5 shows that both 1000 µM or 500 µM Nar significantly impaired the number of closed polygons formed by cells stimulated with VEGF compared with samples stimulated with VEGF alone.

This evidence points out that Nar regulates VEGF-induced capillary-like formation *in vitro* specifically inhibiting the NAADP/TPC2- mediated Ca^{2+} signalling.
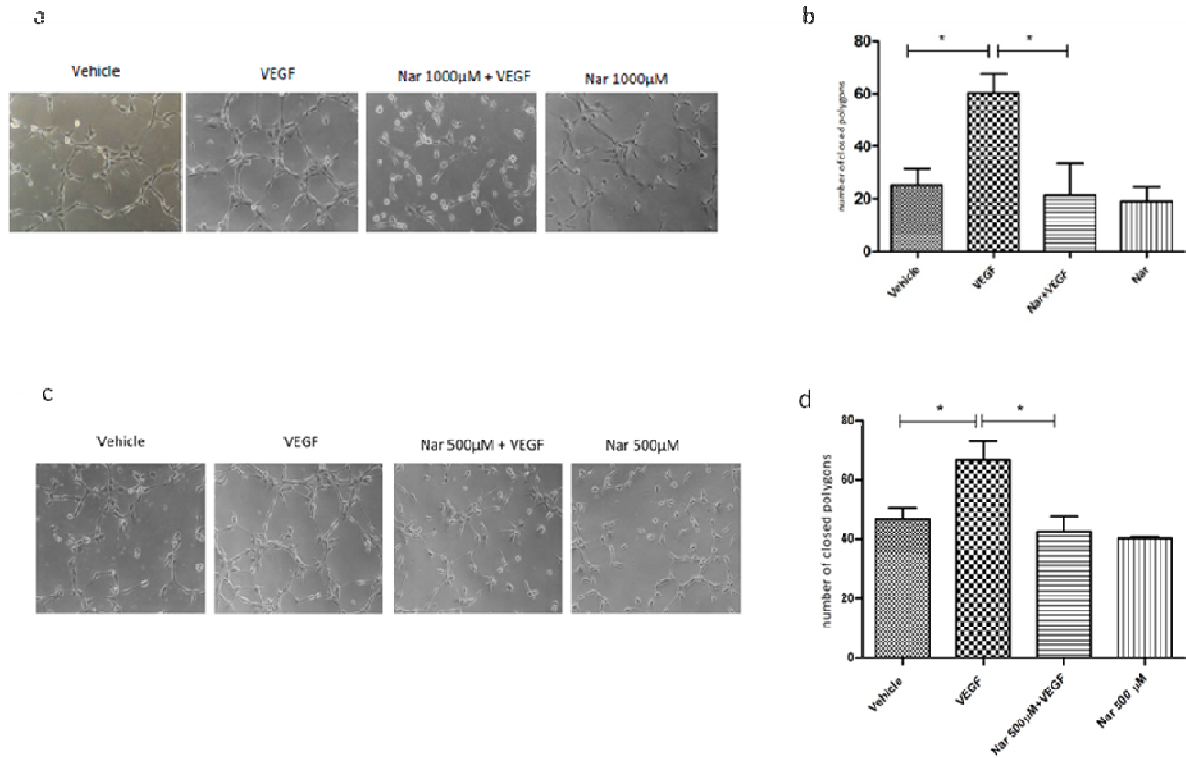
Figure 5. HUVECs ability to form capillary-like structures induced by VEGF *in vitro* were impaired by Naringenin. (a,c) Representative images of one of three independent experiments. HUVECs were plated in Matrigel-coated dishes and incubated for 3–4 h in EBM-2 + 2% FBS supplemented or not with VEGF or Nar 1000 µM (a) and 500 µM (c) or in medium containing both VEGF and Nar. (b,d) Quantitative evaluation of tube formation as the number of closed polygons formed in 6 fields for each experimental condition. Data in bar charts represent mean ± s.e.m. of three independent experiments. $*P < 0.05$

In our *in vivo* murine model we have previously demonstrated that VEGF-treated plugs implanted in the flank of wild type mice not only failed to be vascularized if treated with Ned-19, but more strikingly remained avascular in TPC2 - /- mice. In addition, the

specific role of TPC2 was supported by the evidence that vascularization was not inhibited in plugs from TPC1 -/- mice [1]. To verify the inhibitory effect of Nar on *in vivo* angiogenesis C57BL/6 were injected with matrigel plugs containing either Nar or vehicle, or Nar plus VEGF; five day later the extent of plug vascularization under the different experimental conditions was evaluated by measuring the hemoglobin content. Figure 6 shows that while VEGF alone induces significant vascularization, plugs treated with VEGF plus Nar remain virtually avascular. Interestingly, our observations *in vivo* open a new perspective toward a potential therapeutic approach although we cannot exclude the possibility that targets other than TPC2 may contribute to this antiangiogenic effect.
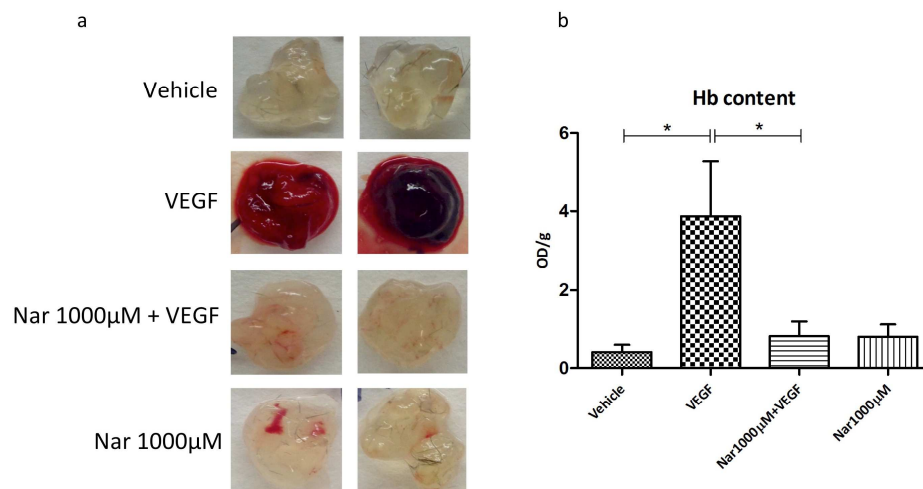

Figure 6. Naringenin affects vascularization induced by VEGF in a *in vivo* murine model. Male/female C57BL/6 mice 5 weeks old were injected subcutaneously with matrigel plugs containing either vehicle or VEGF or VEGF plus 1000 μM Nar. Five days after injection the mice were sacrificed and plug

vascularization was evaluated both macroscopically, as shown in two representative images (a) and as hemoglobin content expressed as absorbance (OD)/1 g matrigel plug (b); values from three independent experiments are expressed as mean ± s.e.m. *$P < 0.05$. $n = 14$–15 plugs for each experimental condition.

4.4 Naringenin does not impair NAADP/TPC2-independent angiogenic responses

We have previously shown and analyzed that intracellular Ca^{2+} signalling is involved in HUVECs angiogenic responses to Angiopoietins. Evidence from pharmacological inhibition of different Ca^{2+} release channels showed that neither the increase of intracellular Ca^{2+} nor the angiogenic responses elicited by Angiopoietin-1 (Ang-1) are dependent on NAADP-TPC2 pathway. In fact, both response were significantly impaired by thapsigargin, which inhibits SERCA pumps, but not by bafilomycin A1, which inhibits pH-dependent Ca^{2+} uptake into acidic stores [5].
To further validate the hypothesis that Nar specifically impairs angiogenic responses inhibiting NAADP/TPC2 signalling pathway we tested Nar effect on HUVECs stimulated with Ang-1, as an angiogenic stimulus that does not couple with TPC2, using Ned-19 as positive control. To this aim calcium imaging experiments were performed. Cells were pretreated for 30 min with Nar (Figure 7a) or Ned-19 (Figure 7b) and stimulated with 100 ng/ml Ang-1. Both Nar and Ned-19 failed to impairs Ang-1-dependent Ca^{2+} mobilization corroborating our aforementioned hypothesis.
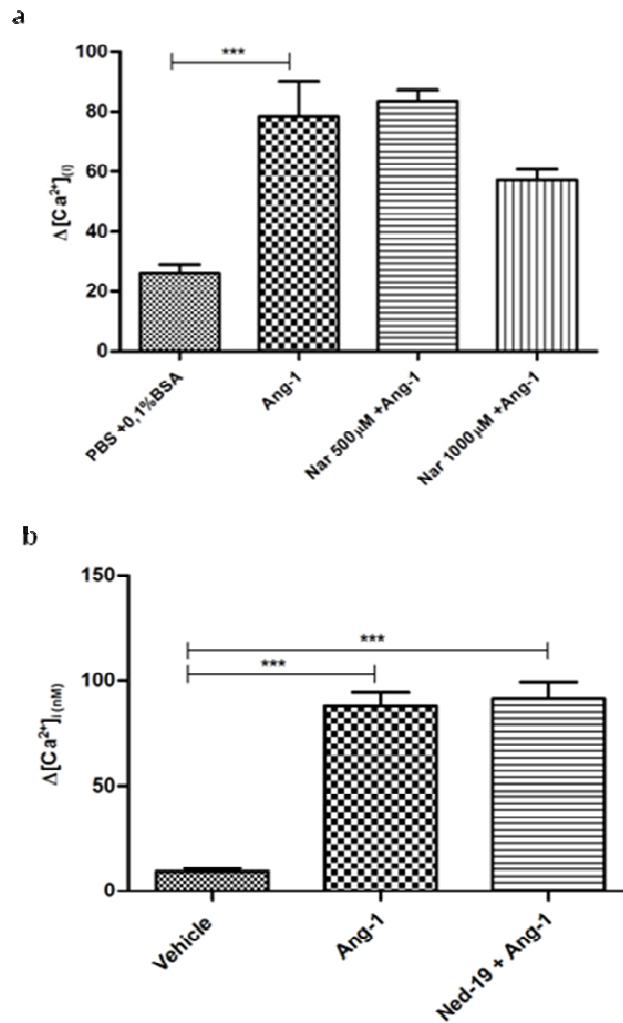
Figure 7. Neither Naringenin nor Ned-19 impairs Ang1-dependent Ca^{2+} release. Live imaging in single FURA2-AM loaded cells. (a) HUVECs were pretreated for 30 min with 500 µM or 1000 µM Nar and then stimulated with 100 ng/ml Ang-1. Both Nar concentrations failed significantly inhibit Ang-1 mediated Ca^{2+} release (P >0,2). (b) Calcium imaging experiments in HUVECs pretreated for 30 min with 100 µM Ned-19 and then stimulated with 100 ng/ml Ang-1. Bar chart

shows that Ang-1induced-increase in $[Ca^{2+}]_i$ is not impaired by Ned-19. Data were from 3 independent experiments ***P<0,001.

Likewise we have analyzed whether Nar was able to impair NAADP/TPC2-independent angiogenic responses *in vitro* and *in vivo*. As expected, Ang-1 stimulated HUVECs capability to form capillary-like structures on matrigel, but both Nar (Figure 8a,b) and Ned-19 (Figure 8c) failed to interfere with this phenomenon *in vitro*.
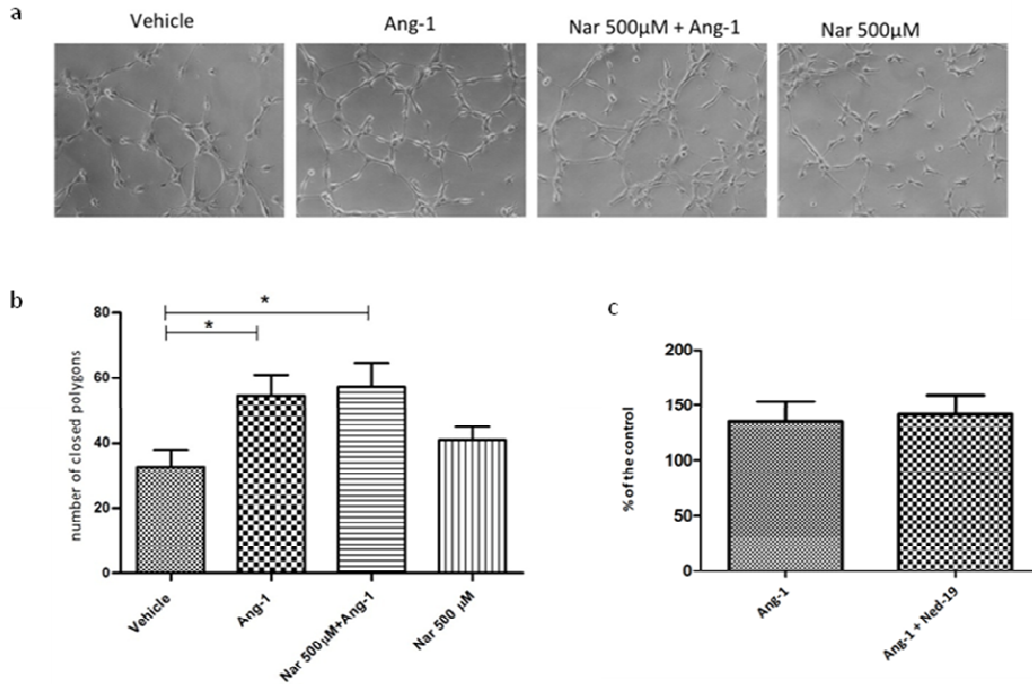
Figure 8. Naringenin does not affect angiogenic responses to Ang-1 *in vitro*. (a) Representative images of one of three independent experiments. HUVECs were plated in Matrigel-coated dishes and incubated for 2–3 h in EGM-2 supplemented or not with Ang-1 or Nar, or in medium containing both Ang-1 and Nar. (b) Quantitative evaluation of tube formation as the number of closed polygons formed in 6 fields for each experimental condition. Data in bar charts represent mean ± s.e.m. of three independent experiments. *$P < 0.05$. (c) Cells were plated in Matrigel-coated dishes and incubated for 2-3 h in EGM-2 supplemented with Ang-1 or Ang-1 + Ned-19. Quantitative evaluation of tube formation as the number of closed polygons formed in 9 fields for each experimental condition. Data in bar charts represent percentage of the control (mean ± s.e.m. of three independent experiments).

In addition *in vivo* matrigel assay were performed. Matrigel plugs containing either Nar or vehicle or Nar plus Ang-1from injected mice were evaluated in hemoglobin content 5 days after inocolum.

Bar charts in Figure 9 show that the vascularization of Ang-1 plugs did not significantly differ from that in Ang-1 plus Nar plugs.

Taken together these data indicate that IP_3-dependent Ca^{2+} responses and angiogenic process (*in vitro* and *in vivo*) stimulated by Ang-1 are not affected by Nar strongly indicating that Nar specifically impairs NAADP/TPC2- dependent signalling pathway.
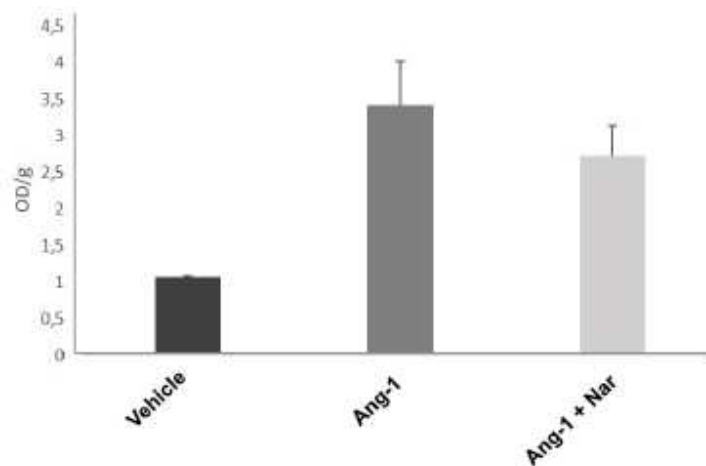
Figure 9. Naringenin does not affect angiogenic responses to Ang-1 *in vivo. In vivo* vessel formation was assessed after subcutaneous injection of 5 weeks old male/female C57BL/6 mice with Matrigel plugs containing either vehicle or Ang-1 (150 ng/ml) or Ang-1 plus 1000 μM Nar. Five days after injection the mice were sacrificed and plug vascularization was evaluated as hemoglobin content expressed as absorbance (OD)/1 g matrigel plug. Hemoglobin content in Ang-1 plugs (n=8) did not significantly differ from that in Ang-1 + Nar plugs (n=8) (P>0.2).

4.5 Conclusions (1)
In the present study we demonstrated that Nar can specifically inhibit the ability of TPC2 to release Ca^{2+} from acidic stores in

NAADP-mediated responses. Electrophysiological analysis shows that hTPC2-current is specifically reduced by Nar. Furthermore, we assess the possible effects of Nar on TPC2 in human endothelial cells analyzing VEGF-dependent Ca^{2+} release and VEGF-dependent angiogenesis *in vitro* and *in vivo*. Both Ca^{2+}-activated responses of HUVECs to VEGF and *in vitro* and *in vivo* angiogenesis are inhibited by Nar. In addition, Ang-1-dependent angiogenic responses, known to be TPC2-independent, are not affected by Nar. Figure 10 describes schematically the specific role of Nar in the control of VEGF-induced angiogenesis, based on present and previous data.
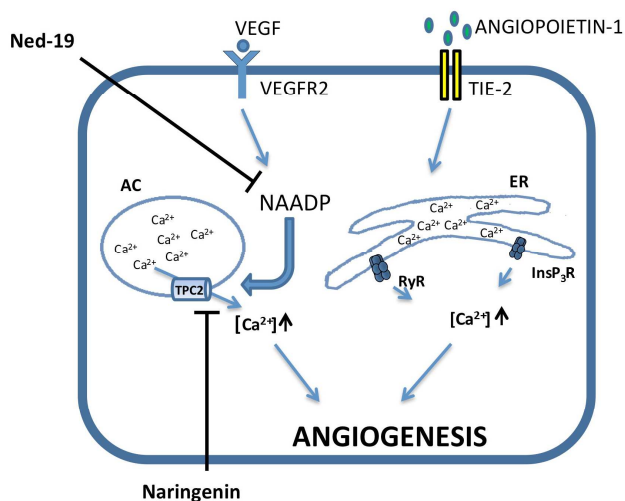
Figure 10. Schematic representation of specific Ca^{+2} signalling pathway involved in the control of angiogenesis by VEGF and Ang-1. Nar inhibits Ca^{+2} mobilization when mediated by TPC2, but not by RyR/InsP₃R. AC: acidic compartments, ER: endoplasmic reticulum.

Besides confirming the inhibitory properties of Nar in VEGF-induced angiogenesis, the data from the present study shed new

light on the mechanisms underlying this process by revealing the pivotal role played by TPC2 and provide the first evidence of the antiangiogenic properties of Nar in an *in vivo* murine model.

Nar is known to exert a wide range of effects induced by a number of mechanisms that have yet to be discovered.

By contrast, a limited number of factors are known to modulate TPC2 activity, and our data shed light on a novel, naturally-occurring molecule that targets this channel which is attracting a considerable amount of interest owing to its relevance to important pathophysiological processes. The relationship we describe here between naringenin and TPC2 is therefore likely to have wider implications in systems other than the vascular system, thus representing a novel tool for experimental, and possibly even clinical, research purposes.

4.6 Naringenin impairs B16 melanoma cells VEGF-dependent Ca^{2+} responses

In tumor biology Ca^{2+} signaling pathway represents an important aspect. Changes in Ca^{2+} toolkit lead cancer cells to acquire some distinctive hallmarks such as alteration in the expression of proteins involved in the mobilization of Ca^{2+} across the plasma membrane and sub-cellular organelles. Many studies have shown that Ca^{2+} is involved in basic processes such as proliferation, migration, survival of tumors cells, invasiveness and metastasis formation [9-12]. On the basis of this evidence we have recently focused our attention on the study of VEGF-dependent Ca^{2+} signaling in cancer cells, starting with murine melanoma. We have demonstrated a role for NAADP-evoked Ca^{2+} signalling in a number of melanoma features *in vitro* and in a murine melanoma *in vivo* model. Using the NAADP inhibitor Ned-19 in B16 melanoma cell line cultured *in vitro* or inoculated in C57BL/6 mice *in vivo* we have observed that NAADP controls cellular migratory ability, cellular proliferation, tumor vascularization, growth and

metastatic dissemination. These data strongly suggest that NAADP/TPC2 Ca^{2+} pathway can be relevant not only for neoangiogenesis, but also for a direct control of tumor cells [2].
Exploiting Nar ability to block TPC2-mediated responses in HUVECs we have investigated whether Nar could interfere with the response of B16 melanoma cells to VEGF. Ca^{2+} imaging experiments were performed in B16 FURA2-AM loaded single cells pretreated for 30 min with different concentrations of Nar and stimulated with 100 ng/ml VEGF. Histograms in Figure 11a, shows that Nar is able to inhibit VEGF-related Ca^{2+} signalling in a dose-dependent manner. Furthermore, to directly assess the specific inhibitory effect of Nar treatment on TPC2 in this experimental system we have performed Ca^{2+} imaging experiments pretreating cells with Nar and stimulating them with 100 nM NAADP-AM. Data in bar charts show that NAADP-mediated Ca^{2+} mobilization is inhibited by Nar, (Figure 11b). In addition, to further support our observation we have also performed Ca^{2+} imaging experiments pretreating cells with different concentration of Ned-19 (previously demonstrated to inhibit NAADP-dependent responses in B16 melanoma cells [2]) and stimulating them with 100 nM NAADP-AM. As expected, Figure 11c shows that also Ned-19 was able to significantly inhibit Ca^{2+} responses to NAADP-AM. Taken as a whole these observations strongly suggest a specific inhibitory effect of Nar on TPC2-mediated Ca^{2+} release also in B16 melanoma cells.
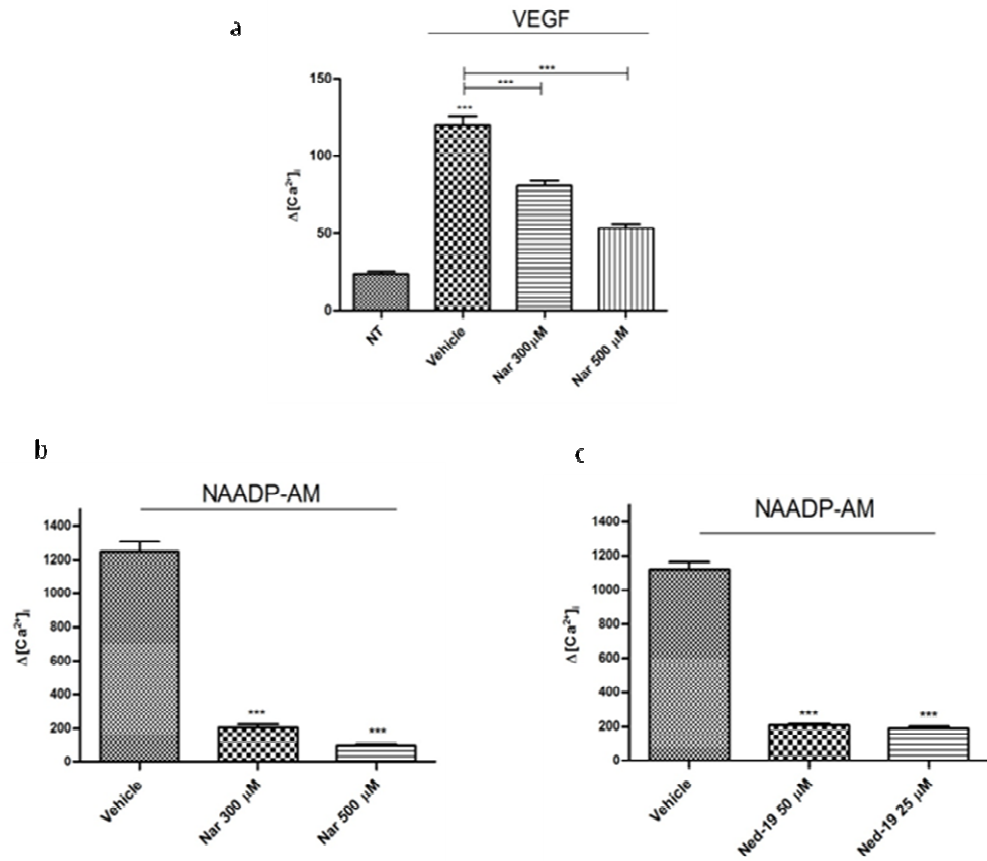
Figure 11. Naringenin inhibits NAADP-controlled Ca^{2+} mobilization in B16 melanoma cells. Ca^{2+} imaging experiments. Cells pretreated for 30 min with different concentration of Nar were stimulated with 100 ng/ml VEGF (a) or 100 nM NAADP-AM (b). (c) B16 cells pretreated with Ned-19 and stimulated with 100 nM NAADP-AM.

4.7 Naringenin affects the proliferative/migratory behavior of B16 melanoma cells

Migration and proliferation are characteristic hallmarks of cancer; we have previously demonstrated that NAADP- mediated Ca^{2+} release is required for the migratory ability of B16 cells in their own conditioned medium. Indeed, we have shown that Ned-19 significantly reduces cells migration and focal adhesion kinase (FAK) activation, protein known to have an important role in the regulation of dynamic changes in actin cytoskeleteon reorganization [2]. In order to investigate the possible inhibitory effect of Nar on B16 melanoma cells migratory ability, scratch assay was performed on confluent monolayers treated or not with the inhibitor and cultured for 18 hours in the absence of serum in order to minimize the contribution of growth versus migration. Figure 12a,b shows that B16 melanoma cells capability to move on the wound is inhibited by Nar. In addition western blot analysis of P-FAK and P-AKT levels at the same time and conditions shows that Nar significantly impairs FAK and AKT activation allowing to attribute, at least in part, the observed behavior to changes in cell motility (Figure 12c,d). This point, of potential relevance for the control of invasive and metastatic behavior, opens the way to further more direct and elaborate approaches, presently ongoing in our laboratory.
We also asked whether in this experiment Nar had interfered with the proliferation. To this purpose cell cycle analysis were performed in the same experimental conditions (18h, no serum) and % G1 and S phase was evaluated in a cytometer. Data in figure 13 a, b show that Nar treatment significantly abates the percentage of cells undergoing S phase and increases the percentage of cells undergoing G1 phase. Analyzing these results we cannot exclude the contribute of proliferation inhibition on the migration process, but this indications suggest that both of them may be affected by Nar. We previously demonstrated in B16 melanoma cells the important role of NAAD/TPC2 mediated responses on the control

of migration and proliferation [2]. Taken together these data suggests that Nar can interfere with this control most likely through TPC2, a hypothesis which we are presently investigating by means of genetic approaches.

a

T=0   T=18

Vehicle

Nar 100 µM

Nar 200 µM

b
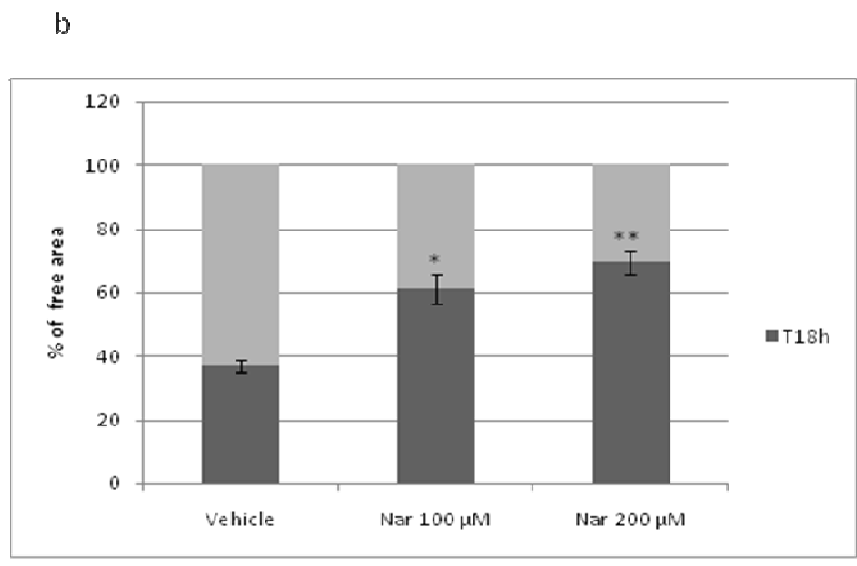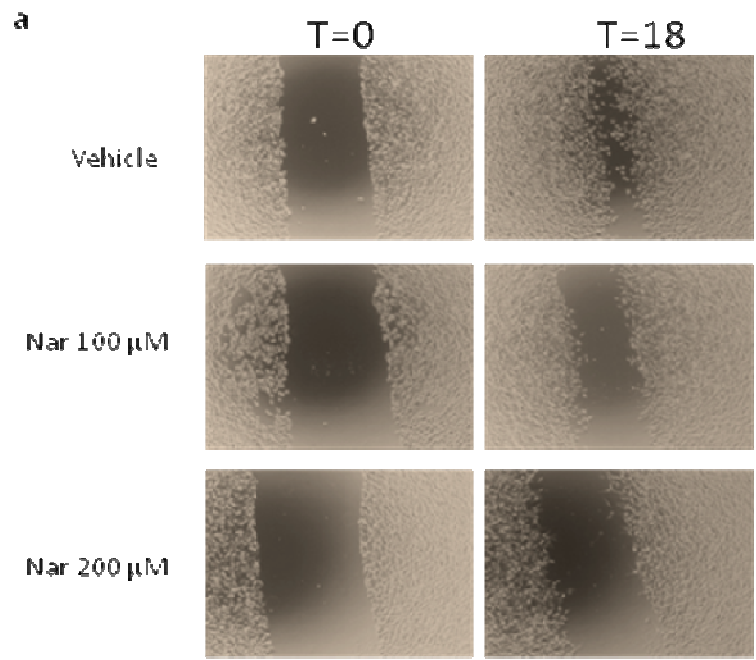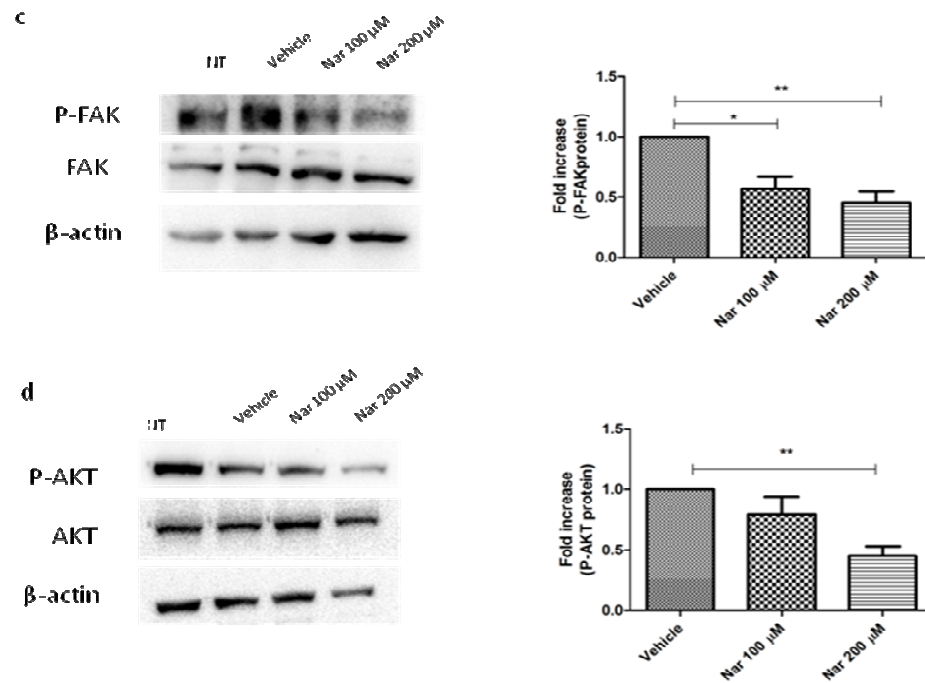
Figure 12. Naringenin impairs melanoma migration. (a) Scratch assay to investigate B16 melanoma cells ability to move on wound. Wounded monolayer were maintained in serum free medium in presence or absence of Nar for 18h. Representative images of three independent experiments at the time of manual damage t=0 and after 18h. (b) Quantitative evaluation of the percentage of free area versus t=0 after 18h. (c,d) Western blot assessment of phosphorylation levels of FAK (c) and AKT (d). Cells, treated or not with Nar in a serum free medium for 18h, were lysed and western blot analysis was performed.
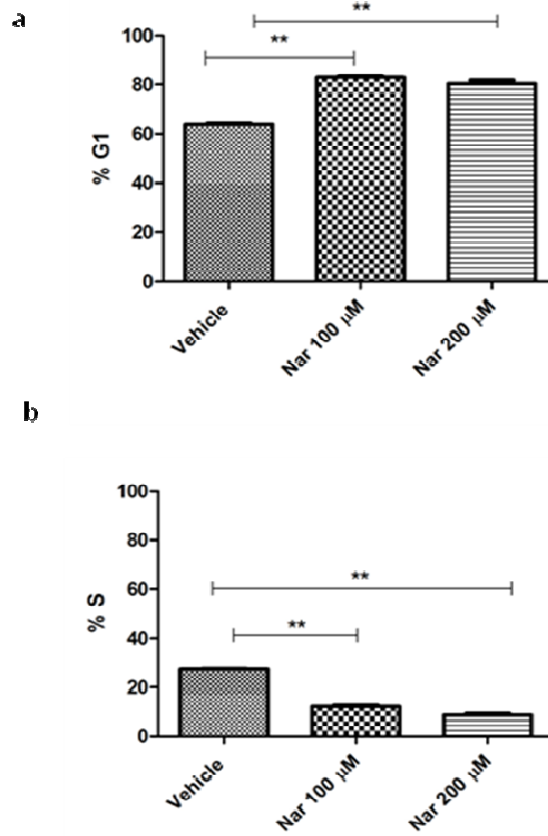
Figure 13. Naringenin interferes with B16 melanoma cell cycle increasing G1phase and decreasing S phase. (a,b) Data are representative of three independent experiments. Evaluation of (a) % G1 phase (b) % S phase 18h after Nar treatment in a serum free medium.

4.8 Naringenin interferes with B16 melanoma ability to form vascular-like tube network

The ability of aggressive tumor cells to form vascular channels, a phenomenon known as vasculogenic mimicry (VM) has been described. Through this process tumor cells, without implication of ECs, form tubes de novo independently of angiogenesis. Interestingly, channels are not true blood vessels formed by preexisting ones, but mimic capillary function. In addition, a link has been highlighted between VM and poor clinical outcomes and suggesting that this could explain why some tumors poorly respond to angiogenic inhibitors [81, 87].

The initial characterization of this tumor plasticity was made in melanoma in which cells coexpression of endothelial, tumor markers and perfusible vascular-like structures rich in laminin, collagens IV and VI and heparin sulfate proteoglycans were described [80]. Furthermore, subsequent comparative studies between melanoma VM networks versus endothelial-dependent angiogenic vasculature reported upregulated expression of key angiogenesis-related and stem-cell–associated genes by the melanoma cells [81].

Interestingly, we have observed that Nar interferes with melanoma cells VM. We have seeded B16 melanoma cells on Matrigel and culturing them for 18h to allow for the development of capillary-like tubes. The cells treated in a serum free medium with the vehicle alone underwent a rearrangement and formed a vasculogenic network within 18h. Otherwise, cells treated with 200 μM Nar showed a significant inhibition of these structures suggesting a possible role for TPC2 in VM, (Figure 14).

In this study we have introduced the natural flavonoid Nar as a tool to directly block TPC2-mediated angiogenic response in HUVECs. In addition, VM of B16 melanoma cells is also impaired by Nar; although we cannot exclude the possibility that in B16 melanoma cells Nar targets pathways different from TPC2, these data suggest that this ion channel may have a possible role in endothelial and melanoma pathways in the formation of angiogenic and non-

angiogenic vascular system respectively: a novel promising field worth of further insight.
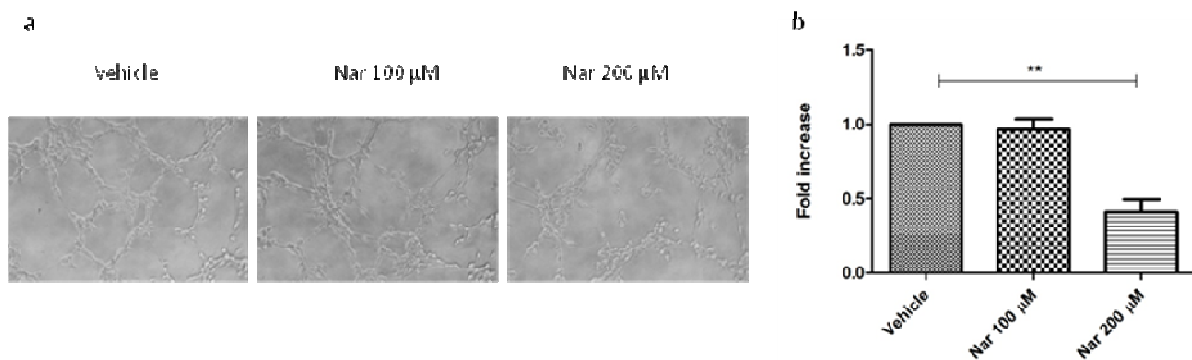
Figure 14. Naringenin inhibits B16 melanoma cells ability to form vascular-like structures. Cells were seeded on Matrigel in presence or absence of Nar in a serum free medium for 18h. (a) Representative images of one of five independent experiments. (b) Quantitative evaluation of tube formation as the number of closed polygons formed in 9 fields for each experimental condition. Data in bar charts represent fold of treated samples compared with control set as 1 (mean ± s.e.m. of five independent experiments).

4.9 Concluding remarks

Investigating cancer behavior in the context of its microenvironment represents an important aspect in the fight against cancer. In particular, angiogenesis has a pivotal role in tumor progression and the communication with the surrounding environment.

In literature several studies point out the emerging role of TPCs in patophysiological processes [1, 42-48] including cancer [2, 49, 50].

Indeed, we have previously demonstrated TPC2 involvement in angiogenesis and NAADP signalling [1, 2].

In this study we introduce Nar as a novel natural pharmacological tool able to interfere with TPC2 activity. In particular, we have demonstrated that in endothelial cells Nar specifically inhibits both VEGF/NAADP/TPC2-dependent Ca^{2+} mobilization and angiogenesis *in vitro* and *in vivo*. On the other side, also data from melanoma, although lacking a direct correlation, strongly suggest that Nar effects on B16 biological processes may be dependent upon TPC2 inhibition.

Finally, on the basis of this evidence, we can conclude that Nar may represent an important natural tool that potentially capable to impair NAADP/TPC2 Ca^{2+} signalling not only in angiogenesis but also in melanoma progression pointing out the relevance, for clinical application, to develop drugs able to target at the same time both processes.

5. MATERIALS AND METHODS

5.1 *Arabidopsis thaliana tpc1–2* mutants [88] were grown in soil in a growth chamber at 22 °C and 8 h light/16 h dark regime. Well-expanded leaves from 4 weeks old plants were used for mesophyll protoplast preparation as described in refs [89] and [90]. The transient transformation was performed as described previously [83, 85] using the pSAT-hTPC2-EGFP or pSAT-hTPC1-EGFP plasmid as reported therein.

The transformed cells were maintained in the dark at 23 °C in W5 ionic solution (in mM: 154 NaCl, 125 $CaCl_2$,KCl 5, MES 2, pH 5.6 with KOH) plus 50 μg/ml Ampicillin as described in ref. [89]. Vacuoles were efficiently released from the protoplasts using the following vacuole release solution (in mM): 100 malic acid, 5 EGTA, $3MgCl_2$, pH 7.5 using 160 1,3-bis (tris(hydroxymethyl)methylamino) propane (BTP), 450 mOsm with D-sorbitol.

5.2 Patch-clamp recordings. Patch-clamp experiments on vacuoles from fluorescent protoplasts expressing the hTPC2-EGFP fusion on the tonoplast were performed in whole-vacuole configuration ≥40 h after the transformation.

The bath solution (cytoplasmic side) contained (in mM): 100 NaCl, 2 $MgCl_2$, 10 Hepes-Tris, pH 7.5. The pipette solution (vacuolar side) was (in mM): 100 NaCl, 2 $MgCl_2$, 10 MES-Tris, pH 5.5. The bath solution and the pipette solution were adjusted to 580 mOsm and 618 mOsm by the addition of D-sorbitol. Dithiothreitol (DTT; 2 mM) was added to the vacuole release solution before the patch-clamp experiments. DTT was prepared as 1 M stock solution the day of the experiment and kept on ice until use. Nar was also prepared fresh as a stock solution in DMSO. Since the usual maximum concentration of Nar used in electrophysiological studies (100 μM) induced about 40% inhibition of hTPC2 and even less of AtTPC1, we decided to increase [Nar] up to 1000 μM. However, some precipitate was present in these conditions possibly slightly reducing the nominal Nar concentration. We also verified

that the maximum DMSO concentration used in this study (up to 0.1%) were not effective on channel activity. PI $(3,5)P_2$, purchased as dioctanyl ester (diC8) from AG Scientific or Echelon Biosciences Inc, was prepared as 1 mM stock solution and stored at −20 °C. The other chemicals were purchased from Sigma-Aldrich and Carl Roth.

5.3 Analysis of electrophysiological data. Positive currents correspond to cations flowing from the cytoplasmic side to the lumen of the vacuole. Data analysis and figure preparation were done with Igor Pro software (Wavemetrics) or Photoshop (Adobe Inc.).

5.4 Cell culture. HUVECs were obtained from Lonza Sales Ldt, cultured in EGM-2 Endothelial Cell Growth Medium-2 (Endothelial Basal Medium EBM-2 + EGM-2 Bullet Kit, Lonza), + 100 mM Penicillin/Streptomycin (P/S) (Sigma); Cells were used at passage 1 to 6.
B16 F0 melanoma cells ATCC CRL-6322 were cultured in Dulbecco's Modified Eagle Medium (DMEM) supplemented by 10% FBS, 2% P/S and 2% L-glutamine (Sigma).
Both cell lines were maintained at 37 °C in a humidified 5% CO_2 incubator.

Reagents used are: VEGF-A165 (Peprotech), Ang-1 (Peprotech), Histamine (Sigma), ATP (Sigma), Ned-19 (Tocris Bioscience) Naringenin (Sigma); NAADP-AM was a generous gift of G. C. Churchill (Oxford University).

5.5 Calcium imaging. Cells were incubated in EGM-2 or DMEM containing 3.5 μM Fura-2-AM (Invitrogen) for 1 h at 37 °C and then rinsed with either Hanks' Balanced Salt Solution (HBSS, Sigma) or Ca^{2+} free Krebs Henseleit Hepes buffer (KHH). Dishes were placed into a culture chamber kept at 37 °C controlled temperature on the stage of an inverted microfluorimeter (Nikon

TE2000E) connected to a cooled CCD camera (512B Cascade, Princeton Instruments). Samples were illuminated alternately at 340 and 380 nm using a random access monochromator (Photon Technology International) and emission was detected using a 510 nm emission filter. Images were acquired (1 ratio image/s) using Metafluor software (Universal Imaging Corporation). Calibration of the signal was obtained at the end of each experiment by maximally increasing intracellular Ca^{2+}-dependent Fura-2 fluorescence ratio (340/380) with 5 μM ionomycin (ionomycin calcium salt from Streptomyces conglobatus, Sigma) followed by recording minimal ratio in Ca^{2+}-free medium. $[Ca^{2+}]_i$ was calculated according to previously described formulas [91].

5.6 Western Blot. HUVECs were first starved in EBM-2 + 2% FBS for 4 h and then incubated with Nar for 30 min or with TSU-68 (SU6668, Selleckchem), an inhibitor of VEGFR2 tyrosine kinase activity, for 1 h before VEGF stimulation for 15 min. The primary antibody used was anti-Phospho-VEGF Receptor 2 (Tyr1175) (Cell Signaling Technology) revealed by Goat Anti-Rabbit IgG (H+L)-HRP Conjugate (BIO-RAD). To ensure equal loading, membranes were reprobed with Monoclonal Anti-α-Tubulin antibody (Sigma) followed by Goat Anti-Mouse IgG (H+L)-HRP Conjugate (BIO-RAD).
B16 F0 seeded the day before, were rinsed twice with PBS and then treated for 18h in serum free medium containing vehicle or different concentrations of Nar. The primary antibody used were Phospho-FAK (Tyr 925) (Cell Signaling Technology), FAK (Cell Signaling Technology), Phospho-AKT (Ser 473) (Cell Signaling Technology), AKT (Cell Signaling Technology). Each antibody has been revealed by Goat Anti-Rabbit IgG (H+L)-HRP Conjugate (BIO-RAD).
The intensity of western blot bands was quantified by Image Lab 5.2.1 software (BIO-RAD) from three independent experiments.

5.7 *In vitro* angiogenesis assay. Capillary-like endothelial tube formation was evaluated by an *in vitro* angiogenesis assay. 130 μl Matrigel Basement membrane Matrix Growth factor Reduced (BD Biosciences) was added to each well of pre-cooled 24-well tissue culture plates. Pipette tips and matrigel solution were kept cold during the procedure to avoid solidification. The plates were incubated for 1 h at 37 °C to allow matrix solution to solidify. 4×10^4 HUVECs in a final volume of 500 μl EBM-2 + 2% FBS were seeded in each matrix-coated well. Cells were pretreated with 500 μM or 1000 μM Nar or with vehicle alone and stimulated with 100 ng/ml VEGF for 3–4 hours at 37 °C. Cells stimulated with 100 ng/ml Ang-1 for 2–3 hours, pretreated with 500 μM Nar or 100 μM Ned-19, were seeded in EGM-2. Tube formation was inspected under an inverted microscope (Nikon Eclipse TS100) and images were acquired by a digital camera (Nikon Ds Fi2, Nis elements F 4.00.00 software). The closed polygons formed in at least six random view microscopic fields per well were counted and values averaged.

5.8 *In vivo* angiogenesis assay. The ability of Nar to modulate VEGF-induced neovascularization was tested by matrigel plug assay. Matrigel (600 μl, BD Biosciences) supplemented with heparin (32 U/ml, Schwarz Pharma S.p.A), VEGF (100 ng/ml, Peprotech) or Angiopoietin1 (150 ng/ml, Peprotech), TNF-α (2 ng/ml, R&D Systems) and ± 1000 μM Nar was injected subcutaneously into C57BL/6 mice flanks where it rapidly formed a gel. The negative controls contained heparin alone, the positive controls heparin plus VEGF and TNF-α. In this assay, cells from the surrounding tissues migrate into the matrigel plug and form vascular structures connected to the mouse blood vessels. After 5 days, mice were sacrificed by CO_2 asphyxia and the angiogenic response was evaluated by macroscopic analysis at necropsy and by measurement of the hemoglobin content in the matrigel plug. Hemoglobin was mechanically extracted in water and measured using the Drabkin method by spectrophotometrical analysis

(Sigma) at 540 nm. The values were expressed as optical density/100 mg matrigel.

The animals were housed in the accredited animal facility of the Department of Anatomy, Histology, Forensic Medicine and Orthopaedics, Unit of Histology and Medical Embryology, Sapienza University of Rome, in individual cages, in an environmentally controlled room (23 °C, 12 h light-dark cycle) and provided with food and water *ad libitum*.

All of the procedures were approved by the Italian Ministry for Health and conducted according to Italian law.

5.9 Scratch Assay. Confluent B16 F0 cells monolayer were scraped along a straight line to create a narrow gap (scratch). Cells were rinsed twice with PBS prior the incubation in serum free medium in the presence or absence of Nar. To record cell migration, images of the wound were acquired at time zero and again 18h later.

5.10 Cell cycle analysis. In 18h cell cycle analysis cells were serum starved. Propidium iodide (PI) staining: cells were detached with trypsin/EDTA and resuspended in phosphate-buffered saline (PBS) plus 50 % FBS and then fixed in 70% ethanol for 24h. After washing three times with PBS cells were incubated with PI/RNAse for 3h at room temperature before FACS analysis using a Coulter Epics XL flow cytometer (Beckman Coulter, Fullerton, CA).

5.11 Vascular-like structure formation: Vasculogenic Mimicry. $2x10^4$ B16 F0 cells per well were seeded onto Matrigel (BD Bioscences) in 96-well plates. Before seeding, cells were resuspended in fresh serum free medium in presence or absence of Nar. The formation of vascular-like tubes was analyzed 18h after plating. The vessel like channels were measured as total number of closed polygons for each areas in each well.
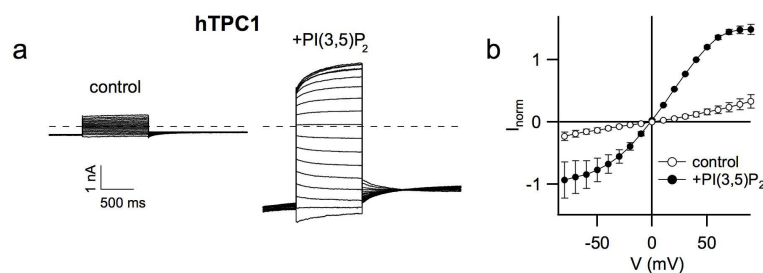
5.12 Statistical analysis. Data are presented as the mean ± s.e.m. of results from at least three independent experiments. Student's t test was used for statistical comparison between means where applicable. *P < 0.05; **P < 0.01; ***P < 0.001.

5.13 Ethical Standards. All the experiments described fully comply with the current laws of Italy

6. APPENDIX

Suppl. Figure 1: the human TPC1 channel is expressed in TPC-free Arabidopsis vacuoles
(a) Currents recorded in the absence (left) and in the presence (right) of 90 nM PI(3,5)P$_2$ added in the cytosolic bath solution. Currents were elicited by voltages ranging to -90 to +80 mV in 10 mV step. Holding and tail voltages were respectively of -70 and -50 mV. (b) Steady-state currents obtained as the mean values of the last 100 ms recording were plotted against the applied voltages. Empty and filled symbols indicated the absence and the presence of 90 nM PI(3,5)P$_2$. Data, shown as mean ± s.e.m., were from 7 different vacuoles.
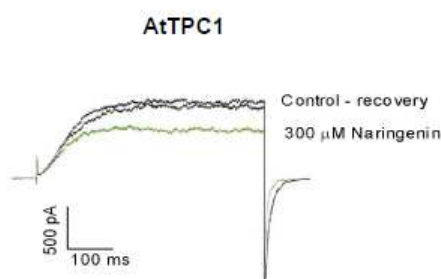
Suppl. Figure 2: Naringenin inhibits the *Arabidopsis thaliana* TPC1
AtTPC1 channel response to voltage stimulation at V= +80 mV in control, in the presence of 300 μM cytosolic Nar and in recovery conditions in vacuoles from mesophyll cells of *Arabidopsis thaliana* plants. Ionic solutions: 200 mM KCl, 2 mM MgCl$_2$, 2 mM CaCl$_2$, 10 mM MES/Tris, pH 5.5 in the pipette; 100 mM KCl, 2 mM MgCl$_2$, 1 mM CaCl$_2$, 1 mM dithiothreitol (DTT), and 10 mM

HEPES/Tris, pH 7.5 in the bath; osmolarity adjusted to 600 mOsm by the addition of D-sorbitol. Similar experiments were performed from at least 15 different vacuoles.

7. REFERENCES

1. Favia, A., et al., *VEGF-induced neoangiogenesis is mediated by NAADP and two-pore channel-2-dependent Ca2+ signaling.* Proc Natl Acad Sci U S A, 2014. **111**(44): p. E4706-15.

2. Favia, A., et al., *NAADP-Dependent Ca(2+) Signaling Controls Melanoma Progression, Metastatic Dissemination and Neoangiogenesis.* Sci Rep, 2016. **6**: p. 18925.

3. Berridge, M.J., P. Lipp, and M.D. Bootman, *The versatility and universality of calcium signalling.* Nat Rev Mol Cell Biol, 2000. **1**(1): p. 11-21.

4. Berridge, M.J., M.D. Bootman, and H.L. Roderick, *Calcium signalling: dynamics, homeostasis and remodelling.* Nat Rev Mol Cell Biol, 2003. **4**(7): p. 517-29.

5. Pafumi, I., et al., *Regulation of Angiogenic Functions by Angiopoietins through Calcium-Dependent Signaling Pathways.* Biomed Res Int, 2015. **2015**: p. 965271.

6. Parrington, J. and R. Tunn, *Ca(2+) signals, NAADP and two-pore channels: role in cellular differentiation.* Acta Physiol (Oxf), 2014. **211**(2): p. 285-96.

7. Stewart, T.A., K.T. Yapa, and G.R. Monteith, *Altered calcium signaling in cancer cells.* Biochim Biophys Acta, 2015. **1848**(10 Pt B): p. 2502-11.

8. Monteith, G.R., et al., *Calcium and cancer: targeting Ca2+ transport.* Nat Rev Cancer, 2007. **7**(7): p. 519-30.

9. Roderick, H.L. and S.J. Cook, *Ca2+ signalling checkpoints in cancer: remodelling Ca2+ for cancer cell proliferation and survival.* Nat Rev Cancer, 2008. **8**(5): p. 361-75.

10. Prevarskaya, N., R. Skryma, and Y. Shuba, *Calcium in tumour metastasis: new roles for known actors.* Nat Rev Cancer, 2011. **11**(8): p. 609-18.

11. Monteith, G.R., F.M. Davis, and S.J. Roberts-Thomson, *Calcium channels and pumps in cancer: changes and consequences.* J Biol Chem, 2012. **287**(38): p. 31666-73.

12. Monteith, G.R., N. Prevarskaya, and S.J. Roberts-Thomson, *The calcium-cancer signalling nexus.* Nat Rev Cancer, 2017. **17**(6): p. 367-380.

13. Clapper, D.L., et al., *Pyridine nucleotide metabolites stimulate calcium release from sea urchin egg microsomes desensitized to inositol trisphosphate.* J Biol Chem, 1987. **262**(20): p. 9561-8.

14. Galione, A., *A primer of NAADP-mediated Ca(2+) signalling: From sea urchin eggs to mammalian cells.* Cell Calcium, 2015. **58**(1): p. 27-47.

15. Raffaello, A., et al., *Calcium at the Center of Cell Signaling: Interplay between Endoplasmic Reticulum, Mitochondria, and Lysosomes.* Trends Biochem Sci, 2016. **41**(12): p. 1035-1049.

16. Ronco, V., et al., *A novel Ca(2)(+)-mediated cross-talk between endoplasmic reticulum and acidic organelles: implications for NAADP-dependent Ca(2)(+) signalling.* Cell Calcium, 2015. **57**(2): p. 89-100.

17. Mojzisova, A., et al., *Effect of nicotinic acid adenine dinucleotide phosphate on ryanodine calcium release channel in heart.* Pflugers Arch, 2001. **441**(5): p. 674-7.

18. Hohenegger, M., et al., *Nicotinic acid-adenine dinucleotide phosphate activates the skeletal muscle ryanodine receptor.* Biochem J, 2002. **367**(Pt 2): p. 423-31.

19. Gerasimenko, J.V., et al., *NAADP mobilizes Ca2+ from a thapsigargin-sensitive store in the nuclear envelope by activating ryanodine receptors.* J Cell Biol, 2003. **163**(2): p. 271-82.

20. Dammermann, W. and A.H. Guse, *Functional ryanodine receptor expression is required for NAADP-mediated local Ca2+ signaling in T-lymphocytes.* J Biol Chem, 2005. **280**(22): p. 21394-9.

21. Gerasimenko, J.V., et al., *NAADP, cADPR and IP3 all release Ca2+ from the endoplasmic reticulum and an*

acidic store in the secretory granule area. J Cell Sci, 2006. **119**(Pt 2): p. 226-38.

22. Steen, M., T. Kirchberger, and A.H. Guse, *NAADP mobilizes calcium from the endoplasmic reticular Ca(2+) store in T-lymphocytes.* J Biol Chem, 2007. **282**(26): p. 18864-71.

23. Lee, H.C. and R. Aarhus, *A derivative of NADP mobilizes calcium stores insensitive to inositol trisphosphate and cyclic ADP-ribose.* J Biol Chem, 1995. **270**(5): p. 2152-7.

24. Churchill, G.C. and A. Galione, *Spatial control of Ca2+ signaling by nicotinic acid adenine dinucleotide phosphate diffusion and gradients.* J Biol Chem, 2000. **275**(49): p. 38687-92.

25. Zhang, F., et al., *TRP-ML1 functions as a lysosomal NAADP-sensitive Ca2+ release channel in coronary arterial myocytes.* J Cell Mol Med, 2009. **13**(9B): p. 3174-85.

26. Lange, I., et al., *Synergistic regulation of endogenous TRPM2 channels by adenine dinucleotides in primary human neutrophils.* Cell Calcium, 2008. **44**(6): p. 604-15.

27. Brailoiu, E., et al., *Essential requirement for two-pore channel 1 in NAADP-mediated calcium signaling.* J Cell Biol, 2009. **186**(2): p. 201-9.

28. Calcraft, P.J., et al., *NAADP mobilizes calcium from acidic organelles through two-pore channels.* Nature, 2009. **459**(7246): p. 596-600.

29. Zong, X., et al., *The two-pore channel TPCN2 mediates NAADP-dependent Ca(2+)-release from lysosomal stores.* Pflugers Arch, 2009. **458**(5): p. 891-9.

30. Zhu, M.X., et al., *Calcium signaling via two-pore channels: local or global, that is the question.* Am J Physiol Cell Physiol, 2010. **298**(3): p. C430-41.

31. Marchant, J.S. and S. Patel, *Two-pore channels at the intersection of endolysosomal membrane traffic.* Biochem Soc Trans, 2015. **43**(3): p. 434-41.

32. Ogunbayo, O.A., et al., *Organelle-specific subunit interactions of the vertebrate two-pore channel family.* J Biol Chem, 2015. **290**(2): p. 1086-95.
33. Galione, A., J. Parrington, and T. Funnell, *Physiological roles of NAADP-mediated Ca2+ signaling.* Sci China Life Sci, 2011. **54**(8): p. 725-32.
34. Morgan, A.J., et al., *Molecular mechanisms of endolysosomal Ca2+ signalling in health and disease.* Biochem J, 2011. **439**(3): p. 349-74.
35. Pitt, S.J., B. Reilly-O'Donnell, and R. Sitsapesan, *Exploring the biophysical evidence that mammalian two-pore channels are NAADP-activated calcium-permeable channels.* J Physiol, 2016. **594**(15): p. 4171-9.
36. Galione, A., *NAADP receptors.* Cold Spring Harb Perspect Biol, 2011. **3**(1): p. a004036.
37. Wang, X., et al., *TPC proteins are phosphoinositide-activated sodium-selective ion channels in endosomes and lysosomes.* Cell, 2012. **151**(2): p. 372-83.
38. Cang, C., et al., *mTOR regulates lysosomal ATP-sensitive two-pore Na(+) channels to adapt to metabolic state.* Cell, 2013. **152**(4): p. 778-790.
39. Ruas, M., et al., *Expression of Ca(2)(+)-permeable two-pore channels rescues NAADP signalling in TPC-deficient cells.* EMBO J, 2015. **34**(13): p. 1743-58.
40. Lin-Moshier, Y., et al., *Photoaffinity labeling of nicotinic acid adenine dinucleotide phosphate (NAADP) targets in mammalian cells.* J Biol Chem, 2012. **287**(4): p. 2296-307.
41. Walseth, T.F., et al., *Photoaffinity labeling of high affinity nicotinic acid adenine dinucleotide phosphate (NAADP)-binding proteins in sea urchin egg.* J Biol Chem, 2012. **287**(4): p. 2308-15.
42. Patel, S., *Function and dysfunction of two-pore channels.* Sci Signal, 2015. **8**(384): p. re7.

43.   Ambrosio, A.L., et al., *TPC2 controls pigmentation by regulating melanosome pH and size.* Proc Natl Acad Sci U S A, 2016. **113**(20): p. 5622-7.

44.   Bellono, N.W., I.E. Escobar, and E. Oancea, *A melanosomal two-pore sodium channel regulates pigmentation.* Sci Rep, 2016. **6**: p. 26570.

45.   Chao, Y.K., et al., *TPC2 polymorphisms associated with a hair pigmentation phenotype in humans result in gain of channel function by independent mechanisms.* Proc Natl Acad Sci U S A, 2017. **114**(41): p. E8595-E8602.

46.   Davidson, S.M., et al., *Inhibition of NAADP signalling on reperfusion protects the heart by preventing lethal calcium oscillations via two-pore channel 1 and opening of the mitochondrial permeability transition pore.* Cardiovasc Res, 2015. **108**(3): p. 357-66.

47.   Hockey, L.N., et al., *Dysregulation of lysosomal morphology by pathogenic LRRK2 is corrected by TPC2 inhibition.* J Cell Sci, 2015. **128**(2): p. 232-8.

48.   Sakurai, Y., et al., *Ebola virus. Two-pore channels control Ebola virus host cell entry and are drug targets for disease treatment.* Science, 2015. **347**(6225): p. 995-8.

49.   Parrington, J., P. Lear, and A. Hachem, *Calcium signals regulated by NAADP and two-pore channels--their role in development, differentiation and cancer.* Int J Dev Biol, 2015. **59**(7-9): p. 341-55.

50.   Nguyen, O.N., et al., *Two-Pore Channel Function Is Crucial for the Migration of Invasive Cancer Cells.* Cancer Res, 2017. **77**(6): p. 1427-1438.

51.   Barreca, D., et al., *Flavanones: Citrus phytochemical with health-promoting properties.* Biofactors, 2017. **43**(4): p. 495-506.

52.   Weng, C.J. and G.C. Yen, *Flavonoids, a ubiquitous dietary phenolic subclass, exert extensive in vitro anti-invasive and in vivo anti-metastatic activities.* Cancer Metastasis Rev, 2012. **31**(1-2): p. 323-51.

53. Giovannucci, E., *Tomatoes, tomato-based products, lycopene, and cancer: review of the epidemiologic literature.* J Natl Cancer Inst, 1999. **91**(4): p. 317-31.
54. Alam, M.A., et al., *Effect of citrus flavonoids, naringin and naringenin, on metabolic syndrome and their mechanisms of action.* Adv Nutr, 2014. **5**(4): p. 404-17.
55. Mir, I.A. and A.B. Tiku, *Chemopreventive and therapeutic potential of "naringenin," a flavanone present in citrus fruits.* Nutr Cancer, 2015. **67**(1): p. 27-42.
56. Li, Q., et al., *Naringenin exerts anti-angiogenic effects in human endothelial cells: Involvement of ERRalpha/VEGF/KDR signaling pathway.* Fitoterapia, 2016. **111**: p. 78-86.
57. Lee, S.H., et al., *Cholesterol-lowering activity of naringenin via inhibition of 3-hydroxy-3-methylglutaryl coenzyme A reductase and acyl coenzyme A:cholesterol acyltransferase in rats.* Ann Nutr Metab, 1999. **43**(3): p. 173-80.
58. Sulfikkarali, N., et al., *Chemopreventive efficacy of naringenin-loaded nanoparticles in 7,12-dimethylbenz(a)anthracene induced experimental oral carcinogenesis.* Pathol Oncol Res, 2013. **19**(2): p. 287-96.
59. Lentini, A., et al., *Enhancement of transglutaminase activity and polyamine depletion in B16-F10 melanoma cells by flavonoids naringenin and hesperitin correlate to reduction of the in vivo metastatic potential.* Amino Acids, 2007. **32**(1): p. 95-100.
60. Abaza, M.S., et al., *Growth inhibitory and chemo-sensitization effects of naringenin, a natural flavanone purified from Thymus vulgaris, on human breast and colorectal cancer.* Cancer Cell Int, 2015. **15**: p. 46.
61. Sun, Y. and J. Gu, *[Study on effect of naringenin in inhibiting migration and invasion of breast cancer cells and its molecular mechanism].* Zhongguo Zhong Yao Za Zhi, 2015. **40**(6): p. 1144-50.

62. Leonardi, T., et al., *Apigenin and naringenin suppress colon carcinogenesis through the aberrant crypt stage in azoxymethane-treated rats.* Exp Biol Med (Maywood), 2010. **235**(6): p. 710-7.

63. Du, G., et al., *Naringenin: a potential immunomodulator for inhibiting lung fibrosis and metastasis.* Cancer Res, 2009. **69**(7): p. 3205-12.

64. Subramanian, P. and D. Arul, *Attenuation of NDEA-induced hepatocarcinogenesis by naringenin in rats.* Cell Biochem Funct, 2013. **31**(6): p. 511-7.

65. Meiyanto, E., A. Hermawan, and Anindyajati, *Natural products for cancer-targeted therapy: citrus flavonoids as potent chemopreventive agents.* Asian Pac J Cancer Prev, 2012. **13**(2): p. 427-36.

66. Bharti, S., et al., *Preclinical evidence for the pharmacological actions of naringin: a review.* Planta Med, 2014. **80**(6): p. 437-51.

67. Saponara, S., et al., *(+/-)-Naringenin as large conductance Ca(2+)-activated K+ (BKCa) channel opener in vascular smooth muscle cells.* Br J Pharmacol, 2006. **149**(8): p. 1013-21.

68. Yang, Z., et al., *Relaxant effect of flavonoid naringenin on contractile activity of rat colonic smooth muscle.* J Ethnopharmacol, 2014. **155**(2): p. 1177-83.

69. Straub, I., et al., *Citrus fruit and fabacea secondary metabolites potently and selectively block TRPM3.* Br J Pharmacol, 2013. **168**(8): p. 1835-50.

70. Vriens, J., B. Nilius, and R. Vennekens, *Herbal compounds and toxins modulating TRP channels.* Curr Neuropharmacol, 2008. **6**(1): p. 79-96.

71. Waheed, A., et al., *Naringenin inhibits the growth of Dictyostelium and MDCK-derived cysts in a TRPP2 (polycystin-2)-dependent manner.* Br J Pharmacol, 2014. **171**(10): p. 2659-70.

72. Adair, T.H. and J.P. Montani, in *Angiogenesis*. 2010: San Rafael (CA).

73. Bergers, G. and L.E. Benjamin, *Tumorigenesis and the angiogenic switch.* Nat Rev Cancer, 2003. **3**(6): p. 401-10.

74. Tahergorabi, Z. and M. Khazaei, *A review on angiogenesis and its assays.* Iran J Basic Med Sci, 2012. **15**(6): p. 1110-26.

75. De Spiegelaere, W., et al., *Intussusceptive angiogenesis: a biologically relevant form of angiogenesis.* J Vasc Res, 2012. **49**(5): p. 390-404.

76. Burri, P.H. and V. Djonov, *Intussusceptive angiogenesis--the alternative to capillary sprouting.* Mol Aspects Med, 2002. **23**(6S): p. S1-27.

77. Ziyad, S. and M.L. Iruela-Arispe, *Molecular mechanisms of tumor angiogenesis.* Genes Cancer, 2011. **2**(12): p. 1085-96.

78. McDonald, D.M. and P.L. Choyke, *Imaging of angiogenesis: from microscope to clinic.* Nat Med, 2003. **9**(6): p. 713-25.

79. Cao, Y., *Future options of anti-angiogenic cancer therapy.* Chin J Cancer, 2016. **35**: p. 21.

80. Hendrix, M.J., et al., *Vasculogenic mimicry and tumour-cell plasticity: lessons from melanoma.* Nat Rev Cancer, 2003. **3**(6): p. 411-21.

81. Hendrix, M.J., et al., *Tumor cell vascular mimicry: Novel targeting opportunity in melanoma.* Pharmacol Ther, 2016. **159**: p. 83-92.

82. Festa, M., L. Lagostena, and A. Carpaneto, *Using the plant vacuole as a biological system to investigate the functional properties of exogenous channels and transporters.* Biochim Biophys Acta, 2016. **1858**(3): p. 607-12.

83. Boccaccio, A., et al., *The phosphoinositide PI(3,5)P(2) mediates activation of mammalian but not plant TPC proteins: functional expression of endolysosomal channels*

in yeast and plant cells. Cell Mol Life Sci, 2014. **71**(21): p. 4275-83.

84.   Jha, A., et al., *Convergent regulation of the lysosomal two-pore channel-2 by Mg(2)(+), NAADP, PI(3,5)P(2) and multiple protein kinases.* EMBO J, 2014. **33**(5): p. 501-11.

85.   Lagostena, L., et al., *The human two-pore channel 1 is modulated by cytosolic and luminal calcium.* Sci Rep, 2017. **7**: p. 43900.

86.   Esposito, B., et al., *NAADP links histamine H1 receptors to secretion of von Willebrand factor in human endothelial cells.* Blood, 2011. **117**(18): p. 4968-77.

87.   Li, S., et al., *The hypoxia-related signaling pathways of vasculogenic mimicry in tumor treatment.* Biomed Pharmacother, 2016. **80**: p. 127-35.

88.   Peiter, E., et al., *The vacuolar Ca2+-activated channel TPC1 regulates germination and stomatal movement.* Nature, 2005. **434**(7031): p. 404-8.

89.   Costa, A., et al., *The Arabidopsis central vacuole as an expression system for intracellular transporters: functional characterization of the Cl-/H+ exchanger CLC-7.* J Physiol, 2012. **590**(15): p. 3421-30.

90.   Yoo, S.D., Y.H. Cho, and J. Sheen, *Arabidopsis mesophyll protoplasts: a versatile cell system for transient gene expression analysis.* Nat Protoc, 2007. **2**(7): p. 1565-72.

91.   Grynkiewicz, G., M. Poenie, and R.Y. Tsien, *A new generation of Ca2+ indicators with greatly improved fluorescence properties.* J Biol Chem, 1985. **260**(6): p. 3440-50.

8. LIST OF PUBLICATIONS

Publications

1- Pafumi I, Favia A, Gambara G, Papacci F, Ziparo E, Palombi F, Filippini A. Regulation of Angiogenic Functions by Angiopoietins through Calcium-Dependent Signaling Pathways. *Biomed Res Int*. 2015 2015:965271. doi: 10.1155/2015/965271.

2- Pafumi I, Festa M, Papacci F, Lagostena L, Giunta C, Gutla V, Cornara L, Favia A, Palombi F, Gambale F, Filippini A, Carpaneto A. Naringenin Impairs Two-Pore Channel 2 Activity And Inhibits VEGF-Induced Angiogenesis. *Sci Rep*. 2017;7(1):5121. doi: 10.1038/s41598-017-04974-1.

Meeting abstracts

1- PAFUMI I, FAVIA A, GAMBARA G, PAPACCI F, ZIPARO E, PALOMBI F, FILIPPINI A. Regulation of Angiogenic Functions by Angiopoietins through Calcium Dependent Signaling Pathways. Workshop SIICA, Certosa di Pontignano (Siena) May 25-27, 2015. Angiogenesi: basi molecolari ed implicazioni terapeutiche V. Abstracts book pag 67.

2- PAPACCI F, PAFUMI I, FAVIA A, PALOMBI F, FESTA M, CARPANETO A, FILIPPINI A. Unravelling calcium signalling complexity during angiogenesis: a novel inhibitor of two-pore channel 2. ABCD Congress, Bologna 21-23 September 2017. Abstracts book pag 195.

3- PAPACCI F, PAFUMI I, FAVIA A, PALOMBI F, FESTA M, CARPANETO A, FILIPPINI A. Naringenin as a novel inhibitor of Two-Pore Channel 2 controlling the angiogenic process *in vitro* and *in vivo*. 71th Meeting of the Italian Society of Anatomy and Histology. Taormina 20-22

september 2017. IJAE Vol 122, n.1(Supplement): 161, 2017.